AN EXPERIMENTAL TECHNIQUE FOR THE STUDY OF ENHANCED HEAT TRANSFER DUE TO MOTION OF A PARTICLE IN THE PROXIMITY OF THE TRANSFER SURFACE

A Thesis Submitted
in Partial Fulfilment of the Requirements
for the Degree of

MASTER OF TECHNOLOGY

By

MRINAL KUMAR BANDYOPADHYAY

to the

DEPARTMENT OF CHEMICAL ENGINEERING

INDIAN INSTITUTE OF TECHNOLOGY KANPUR

APRIL, 1984

CERTIFICATE

This is to certify that the present work ' An experimental technique for the study of enhanced heat transfer due to motion of a particle in the proximity of the transfer surface ' has been carried out under my supervision and has not been submitted elsewhere for a degree.

Dated: 11/4/'84

(D.P. RAO)
Assistant Professor
Department of Chemical Engineering
Indian Institute of Technology
Kanpur - 208016, India

ACKNOWLEDGEMENT

I take this opportunity to extend my sincere thanks to Dr. D.P. Rao, my thesis supervisor for his invaluable and sympathetic guidance at every stage of this work.

I also express my deep sense of appreciation and gratitude to Prof. R.N. Biswas of Electrical Engineering Department for kindly designing the electronic controller circuit for me and providing me with necessary equipments during experimental run. His valuable suggestions and discussions relating to controller circuit are gratefully acknowledged.

I would like to acknowledge with deep gratitude the co-operation and help I received from Dr. D. Bahadur, Mr. D. Ray and Mr. B. Chakraborty of A.C.M.S. during fabrication and mounting of the Film-Sensor-Heater.

I would like to thank Dr. A. Ghosh of Metallurgical Engineering Department and Mr. J.N. Sharma of Glass blowing shop for providing me with rare substrates for the Film-Sensor-Heater and materials for special die fabrication.

I would like to thank Mr. A. Atryay and Mr. R.A. Sharma of Central Workshop, Mr. B.K. Srivastava of precision workshop and Mr. Sanjiva Rao of Chemical Engineering workshop for their

excellent craftmanship. I also thank Mr. R.P. Yadav for his cooperation and help at the last phase of this work.

Help extended by Mr. A. Gupta of Semiconductor Lab., Dr. S.K. Sur and Mr. S. Mishra of Chemistry Department in procuring materials and valuable instruments is gratefully acknowledged.

Thanks are extended to M/S A. Ramakrishna, S.K. Labh, S. Kundu, N. Sharma, S.K. Das, M. Pramanik, A.K. Guha, R. Basu, S.C. Maiti, M. Chatterjee, S. Islam, O.P. Rama and M. Muralikrishna for their assistance whenever needed.

Special thanks to Mr. A.K. Verma for his active help and valuable suggestions throughout my thesis work.

Untiring help rendered by Mr. K.M.S. Prasad of Energy Transfer Laboratory at every stage of this work is unforgettable.

I'd also like to thank Mr. M.M. Beg for typing, Mr. A. Ganguly for drawing and Mr. D.B. Chakraborty for photocopying.

Mrinal Kumar Bandyopadhyay

TABLE OF CONTENTS

LIST OF FIGURES

LIST OF PHOTOGRAPHS

LIST OF TABLES

NOMENCLATURE

A = Area of the film, m^2

A_1 = Voltage gain of op amp stage

A_2 = Voltage gain of differential amplifier stage

Bi = Biot number = $\frac{h_p r_p}{K_{particle}}$

C_p = Specific heat, J/kg.k

d = Particle diameter, m

F_o = Fourier number = $\frac{\alpha \theta}{r_p^2}$

g = Acceleration due to gravity, m/s^2

Gr = Grashof number = $\frac{l^3 \rho_{fluid}^2 g \beta \Delta T}{\mu_{fluid}^2}$

$h(s)$ = Heat transfer coefficient from film at steady state, $w/m^2.k$

$h(t)$ = Heat transfer coefficient from film in transient condition, $w/m^2.k$

h_p = Heat transfer coefficient from fluid to particle, $w/m^2.k$

k = A constant chosen on bridge sensitivity consideration

K = Thermal conductivity at average temperature $(\frac{T_f + T_b}{2})$ w/m.k

l = Width of the film, m

m = Mass of the film, kg

Nu = Nusselt number = $\frac{h(s)l}{K_{fluid}}$

P_e = Additional power input to the FSH in transient state, w

P_{eo} = Additional power input to the FSH at steady state, w

Pr = Pradtl number = $\frac{\mu_{fluid} C_{p\,fluid}}{K_{fluid}}$ at average temperature

$\dot{Q}_c(s)$ = Rate of heat loss by convection at steady state, w

$\dot{Q}_g(s)$ = Rate of heat generation within the film at steady state, w

$\dot{Q}_k$ = Rate of heat loss by conduction at any time, w

$\dot{Q}_c(t)$ = Rate of heat loss by convection in transient state, w

$\dot{Q}_g(t)$ = Rate of heat generation in transient state, w

$\dot{Q}_k(t)$ = Rate of heat loss by conduction in transient state, w

Q_{fc} = Fluid convective transfer term, J

Q_p = Particle convective transfer term, J

Q_t = Total enhanced heat transfer by convection, J

r_p = Radius of the particle, m

R_1 = Bridge arm resistance, ohm

R_2 = Bridge arm resistance in series with the FSH, ohm

R_4 = Bridge arm resistance, ohm

R_{POT} = Variable bridge arm resistance, ohm

R_p = FSH resistance, ohm

Re = Reynolds number = $\frac{d.V_{p\ fluid}}{\mu_{fluid}}$

R_s = $(R_{POT} + R_4)$, ohm

R_o = FSH resistance at initial state, ohm

δR = Small change in resistance due to particle movement, ohm

T = Operating temperature of the FSH, °C

Tm = Mean temperature of fluid inside boundary layer, °C

T_b = Bulk temperature of fluid, °C

T_f = Film temperature, °C

T_o = Initial temperature of the FSH, °C

δT = Small change in temperature of the FSH due to particle movement, °C

ΔT = Temperature difference $(T_f - T_b)$, °C

t = time, s

t_p = total transient period, s

V_a = Bridge output voltage, v

V_b = Bridge output voltage, v

V_e = Bridge excitation voltage in transient state, v

V_{eo} = Bridge excitation voltage at steady state, v

V_o = Op amp output voltage, v

V_p = Particle velocity, s

Greek Letters

α = Thermal diffusivity, m^2/s

α_o = Temperature coefficient of resistance of the film material, ohm/ohm/°C

β = Coefficient of thermal expansion of fluid, 1/K

ρ = Density of the fluid at average temperature, kg/m^3

μ = Viscosity of the fluid at average temperature, kg/m.s

θ = Residence time of the particle, s

ABSTRACT

An experimental technique for studying the nature of enhancement in heat transfer due to a moving spherical particle through a thermal boundary layer has been developed. A constant temperature film-sensor-heater and a mechanism for movement of a particle embedded with a thermocouple at a constant distance from the wall have been developed for this study. The relative contributions of the particle and fluid convective transfer have been determined at different particle to wall distances in air and water using this setup. This technique can be applied for understanding the mechanism of heat transfer in gas and liquid fluidized beds.

CHAPTER - 1

INTRODUCTION

The understanding of the effect of motion of a spherical particle through a thermal boundary layer formed due to fluid flow over a heated flat plate is of great importance for furnishing a framework for studies on the mechanism of wall to bed heat transfer in fluidized beds, slurry reactors and enhanced heat transfer due to turbulent promoters.

The wall to bed convective heat transfer in fluidized beds is generally considered to take place through two parallel modes, namely the particle convective transfer and the fluid convective transfer. In the former mode of transfer it is assumed that a particle arrives at the transfer surface from the core and picks up thermal energy from the surrounding fluid and then returns to the bed where it loses its thermal energy. In the latter mode of transfer, however, heat transfer is assumed to take place through a reduced thermal boundary layer (due to scouring by the particle) adjacent to the transfer surface.

Very few experimental investigations have been reported on the relative contributions of the particle and fluid convective transfer toward the total convective heat transfer in fluidized beds.

A brief summary of the literature is presented below:

Heat transfer from wall to bed has been reviewed by Leva [10] Zenz and Othmer [24], Zabrodsky [23], Kunii and Levenspiel [9], Gelprin and Einstein [6], Botterill [3], Gutfinger and Abuaf [7], Saxena et al [17] and recently by Saxena and Gabor [18].

Mickley and Fairbanks [12] proposed a model similar to the well known surface renewal model in which they assumed a packet of particles would arrive at the wall and pick up energy by unsteady heat conduction and return to the bed. This model has been extensively refined by other workers. In these models it has been generally presumed that the fluid convective transfer is negligible.

Zeigler et al [25] studied simultaneous heat and mass transfer rate from a wet celite sphere. Using the heat and mass transfer analogy they showed that the fluid convective transfer is negligible (5-10%). Baskakov and Suprun [2] also used heat and mass transfer analogy in their study on mass transfer from a naphthalene cylinder and showed that the relative contribution of the fluid convection transfer increases from 10% to 90% as the particle diameter increases from 1 mm. to 4 mm. Zabrodsky et al [22] stressed the need to consider the depence of gas convective term on fluid velocity and assumed it to be proportional to $U^{0.2}$ where U is the superficial gas velocity.

Rao [14] has shown the possibility of estimating heat transfer in the fluidized bed conditions from a knowledge of the role of a moving particle through thermal boundary layer and the particle number density fluctuations near the transfer surface. Subramanian et al [19] experimentally investigated the role of a single particle near heated flat plate and computed the particle pickup, but fluid convective term could not be determined in their method.

Washmund and Smith [21] in their experimental study showed that heat transport by particle convection is insignificant in liquid fluidized beds except possibly at low porosities.

As the fluidized bed combustors, in which particles greater than 1 mm. are used came into prominance, a few attempts were made to model this mode of transfer. Based on the boundary layer analysis within interstitial channels adjacent to wall Adams and Welty [1] proposed a method to estimate the gas convective component in gas fluidized beds. Ganzha et al [5] estimated gas convective component by considering that the turbulent boundary layer is disrupted at the front half of the particle and is reformed within the wake. In the beds where fluid convective transfer is significant the bed behaviour is particulate in nature. Thus, in modelling

the fluid convective transfer the effect of a single particle is to be considered. To understand the nature of disturbance created by a single particle experimental studies are warranted. Such studies are not available in literature.

The objective of the present work was to develop an experimental technique for determination of the nature of enhancement in fluid convective transfer and evaluation of the relative fractions of the particle and fluid convective transfer toward the total heat transfer as a sphere moved through a thermal boundary layer. The experimental apparatus developed for this work consisted of a platinum film sensor cum heater which could be kept at a constant temperature by means of a negative feedback controller and a spherical particle embedded with thermocouple. The particle convective term and the fluid convective term were determined from the responses of the thermocouple and the controller.

Chapter 2 of this thesis presents the experimental technique developed for measurement of particle and fluid convective transfer, fabrication of instruments, calibration and experimental procedure.

Chapter 3 presents the experimental results and discussion of results.

Chapter 4 presents the conclusion of the present work and suggessions for future work.

CHAPTER - 2

EXPERIMENTAL TECHNIQUE AND SETUP

2.1. General

The design of the constant temperature film-sensor-heater is based on the following proposed mechanism:

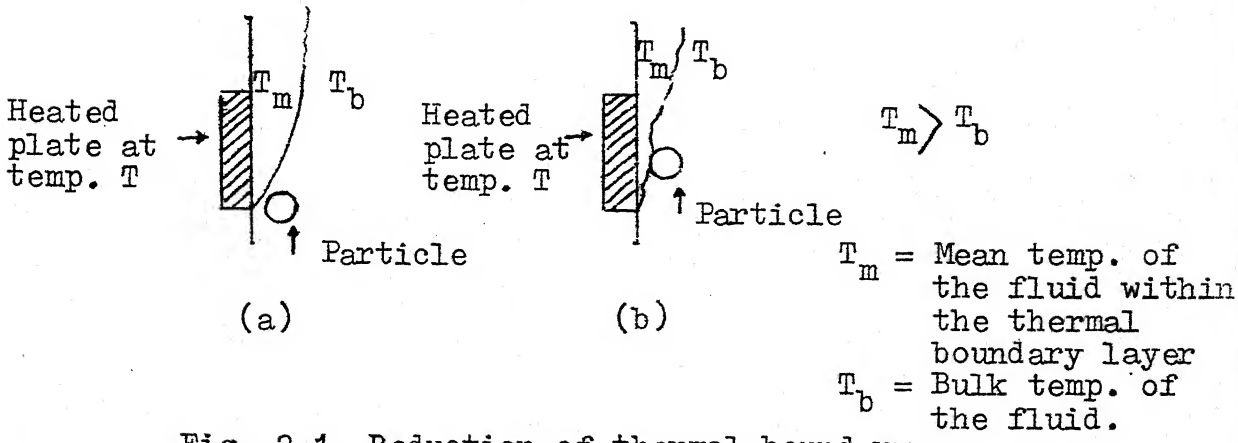

Fig. 2.1. Reduction of thermal boundary layer thickness due to scouring by the particle.

Consider a heated flat plate at temperature T in a fluid medium. At steady state the thermal boundary layer will develop near the surface as shown in figure 2.1(a). Whenever a particle sweeps past the surface through the thermal boundary layer it takes away some energy along with the drifted fluid.

In addition to this, the movement of the particle enhances the heat transfer rate from the surface to the surrounding fluids as the particle scours the thermal layer [figure 2.1(b)]. As a consequense, the surface temperature decreases. If, by some means, the temperature of the surface can be maintained constant despite ~~its~~ the variation in heat transfer rate by supplying additional energy which the surface loses during transient period, then this extra energy supplied will be a measure of the enhanced heat loss from the surface. In other words, the amount of energy supplied, Q_t, to the plate during entire transient period will be equal to the amount of energy picked up by the particle, Q_p, plus the amount of energy transferred to the fluid by convection, Q_{fc}. The terms Q_p and Q_{fc} are also known as the particle convective term and the fluid convective term respectively.

Thus,

$$Q_t = Q_p + Q_{fc} \qquad (2.1)$$

In the actual experiment, an electrically heated metal film sensor (on a suitable substrate) with an arrangement for keeping it at a constant temperature by means of an electronic controller served the purpose of a heated flat plate and a spherical copper bead with embedded copper-constantan thermocouple in it served the purpose of a particle. As the metal film acts as a resistance temperature transducer as

well as a heater, this has, henceforth, been referred to as film-sensor-heater (FSH).

2.2. An expression for evaluation of Q_t

Whenever current is passed through a metal film deposited on a substrate, its temperature increases due to the Joulean heating and depending upon the temperature coefficient of resistance (TCR) its resistance also increases. For a steady power supply the film temperature quickly attains a steady state value because of its negligible mass.

When the particle sweeps past the hot FSH, the one dimensional unsteady state energy balance equation for the film in absence of radiation may be written as

$$\dot{Q}_g(t) = \dot{Q}_c(t) + \dot{Q}_k(t) + mC_p \frac{dt_f}{dt} \qquad (2.2)$$

where

$\dot{Q}_g$ = rate of heat generation within the film

$\dot{Q}_c$ = rate of heat loss by convection

$\dot{Q}_k$ = rate of heat loss by conduction (to the substrat

m = mass of the film material

C_p = specific heat of the film material

$\frac{dt_f}{dt}$ = time rate of change of film temperature

The last term in R.H.S. of equation 2.2 is the accumulation term within the resistive material (metal film). If the film is maintained at a constant mean temperature independent of its heat transfer variation rate, then, $\frac{dt_f}{dt} = 0$.

Elemination of accumulation term is equivalent to making the time constant of the FSH zero [16]. In other words the FSH can respond instantaneously to fluctuations in heat transfer. In addition to the constant film temperature if the thermal penetration depth is also small compared to the substrate thickness then the term $\dot{Q}_k$ may be assumed to be constant with respect to time. Hence equation 2.2 reduces to:

$$\dot{Q}_g(t) = \dot{Q}_c(t) + \dot{Q}_k \qquad (2.3)$$

Therefore, any change in $\dot{Q}_c(t)$ will be reflected in $\dot{Q}_g(t)$. On the otherhand, the one dimensional steady state energy balance equation for the film is:

$$\dot{Q}_g(s) = \dot{Q}_c(s) + \dot{Q}_k \qquad (2.4)$$

The extra amount of heat generated during the entire transient process can be found by subtracting equation 2.4 from equation 2.3 and integrating the resultant expression with respect to time over the transient

period, t_p.

Thus, $$\int_0^{t_p} [\dot{Q}_g(t) - \dot{Q}_g(s)]\,dt = \int_0^{t_p} [\dot{Q}_c(t) - \dot{Q}_c(s)]\,dt \quad (2.5)$$

The L.H.S. of equation 2.5 represents the additional energy supplied (generated through increased power supply) to the FSH for keeping its temperature at a constant level while the R.H.S. represents the total amount of improved heat convected due to the particle movement. Combining equations 2.1 and 2.5 the following expression is obtained:

$$Q_t = \int_0^{t_p} [\dot{Q}_g(t) - \dot{Q}_g(s)]\,dt = Q_p + Q_{fc} \quad (2.6)$$

The quantity $\int_0^{t_p} [\dot{Q}_g(t) - \dot{Q}_g(s)]\,dt$ can be computed directly from the response of the FSH.

2.3 FSH Construction technique

Size of FSH:

As the effect of particle on a flat surface is restricted to within one diameter of its size on both sides of its central position [20] the horizontal dimension (length) of the heater surface has to be 3d plus allowances for leadwire connections, where d is the particle diameter.

For vertical dimension (width), however, no precise norm can be given. If the width is too large the effect due to particle movement will be masked, leading to a large error in Q_t. On the other hand a small width will be inadequate to form an appreciably thick thermal boundary layer. Based on these considerations a width of 0.5 cm and a length of 2.65 cm were chosen for the FSH.

Film material and fabrication:

In theory any material could be used for the preparation of film-sensor-heater. In practice, however, the choice is limited to a very few metals like Pt, Au and Ag due to the nonavailability of convenient means of making films and nonlinearity in TCR [16,4]. Platinum was used as the film material for this sensor and firing technique for film making was adopted instead of evaporation technique because of the practical difficulties.

A liquid platinum paint (liquid bright platinum 05 - x containing platinic chloride and flux dissolved in oil vehicle [16]) was coated on a roughened pyrex glass substrate of 2.65 cm x 0.5 cm x 0.25 cm. The roughening of the substrate was done with SiC paste before coating the paint. The coated substrate was then fired to a temperature of 530 $\pm$ 10°C in a ventilated tube

furnace followed by a slow cooling to room temperature. In the firing process the platinic chloride was reduced to pure metal and was fused to the substrate. Although, the exact chemical nature of the resultant fusion is not clearly known, the film retains the same TCR of platinum metal [11] . The resistance of the film was controlled by the thickness and size of the film layer. The thickness was controlled by the number of coats of film paint that were fired. Before each firing cycle the resistance of the film was checked. The films made in this way were found to be stable with reproducible resistances.

In making the FSH a trial and error method was adopted for selecting the best match among available substrates, surface preperation technique, temperature and firing technique for this particular paint.

Among the various substrates tried (Alumina, ordinary borosilicate glass, pyrex glass) pyrex was found to be the best substrate for 05-x platinum paint. The painted film adhered best on a less highly polished surface, this mostly was due to the stress in the film on cooling and unequal expansion of the metal film and glass. Heating in a ventilated as well as closed furnace was

tried. Inadequate ventilation produced fragile films. A temperature range of 400°C to 650°C was used. Below 400°C the film adherence was poor and above 580°C the glass substrate was softened. A high rate of heating produced unstable fragile films. A moderate heating rate (530 ± 10°C should reach within 2½ to 3 hours) was found to be satisfactory.

Heat treatment

The film-sensor-heaters electrical characteristics were then stabilized by heating them to a temperature of 530 ± 10°C and maintaining that temperature for about 4 hours. Two such cycles were repeated for each sensor. The annealing effect of the firing cycle stabilized the resistance temperature characteristics [13]. The resistances of the prepared film-sensor-heaters were checked frequently at 2-3 days interval after mounting them on the perspex walls. They were heated by passing current (0.01 - 1 amp) through them and were allowed to be cooled and the resistances were then checked again. After 2-3 cycles, the resistances were found to be stable and reproducible. The range of resistances were from 25 ohms to 40 ohms for different sensors.

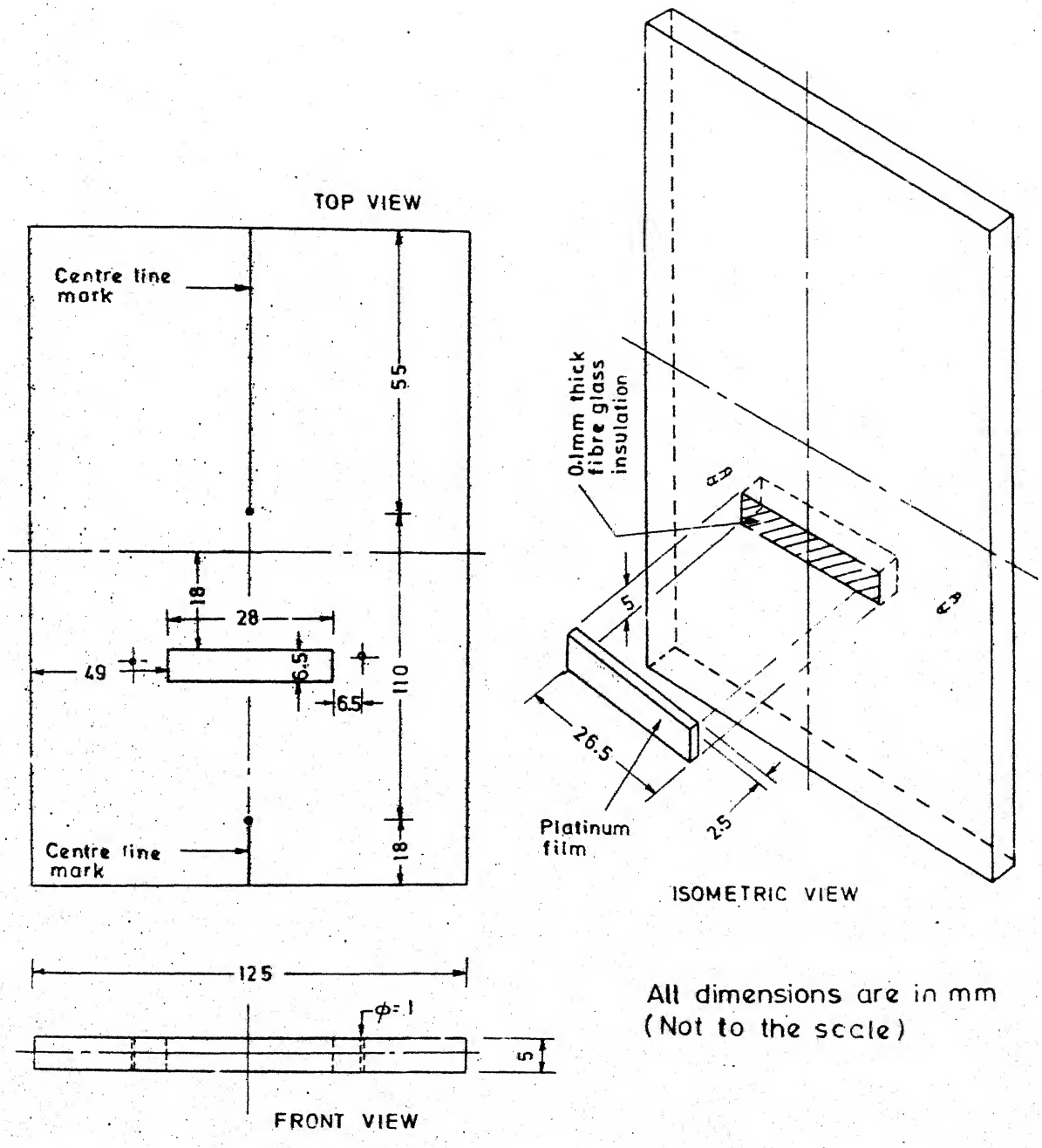

Fig. 2.2 Details of film-sensor-heater mounting on wall

Mounting and lead wire connections

The FSH was flush mounted on to a perspex wall (18.5 cm x 12.5 cm x 0.5 cm). The slot on the wall was made slightly bigger and a thin fibre glass insulation was applied on the inner surfaces of the slot as shown in figure 2.2. The sensor was then tight fitted into the slot and was fixed by applying quickfix from the backside.

A special solder and flux combination was employed for soldering the lead wires on the film and glass substrate. After soldering the lead wires silver paste was applied on to it and allowed to be dried.

This method of fixing minimised the contact resistance to almost zero value. The connecting points were then coated with an epoxy resin. The details are shown in figure 2.3.

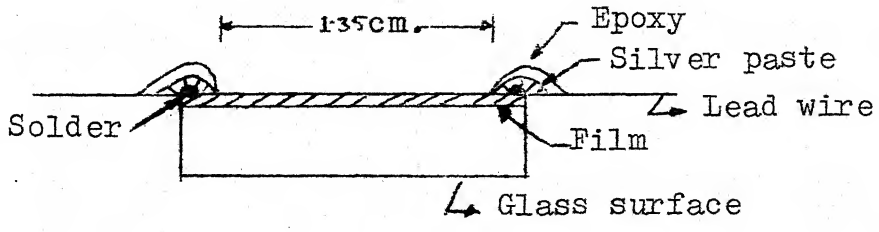

Fig. 2.3. Lead wire connections for the FSH

An approximate composition of the solder and flux employed are given below:

Solder			Flux		
In	-	80-82%	$Zncl_2$	-	3 parts by weight
Pb	-	8 - 10%	NH_4Cl	-	1 part by weight
Sn	-	7 - 8%			
Bi	-	2 - 3%			

The flux was prepared by adding suitable quantity of water. A low temperature was used during soldering (120-140V was applied to a 10W, 250V iron).
The lead wires were then connected to the electronic controller described in section 2.4.

2.4 The electronic controller

The primary function of the electronic control circuit shown in figure 2.4 is to maintain the FSH at a constant temperature. The FSH is, therefore, placed as one arm of a wheatstone bridge which has a provision for adjusting the temperature of the sensor heater for bridge balance by means of a tenturn potentiometer (R_{POT} in figure 2.4). As the temperature of the sensor heater would depend on the bridge excitation voltage, Ve, this voltage is made to depend in an appropriate fashion on the bridge unbalance voltage ($V_b - V_a$) through a differential input

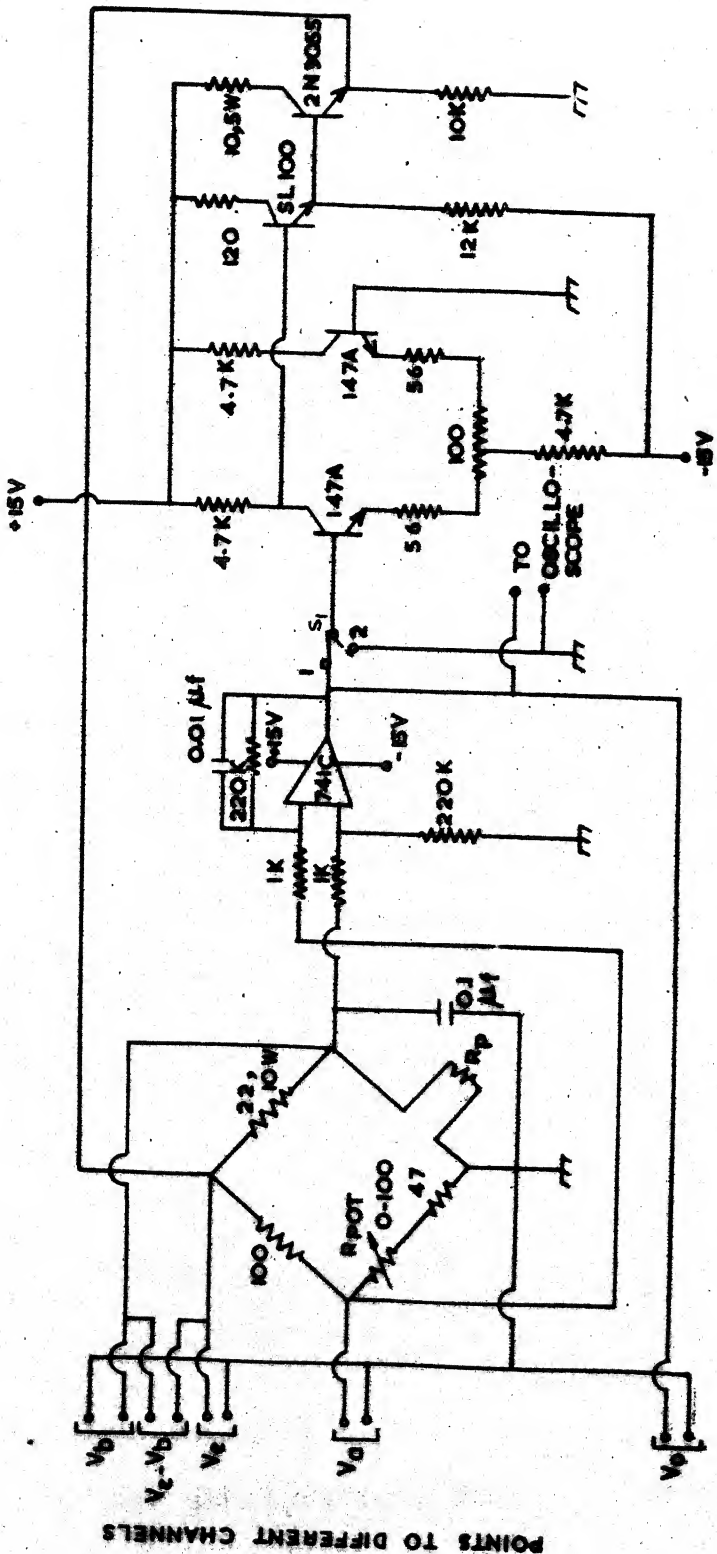

Fig. 2.4 Electronic controller circuit and connection diagram

amplifier so as to constitute an overall negative feedback leading to a zero unbalanced voltage and hence a constant temperature of the sensor heater.

Obviously, a certain magnitude of this bridge excitation voltage has to be maintained even when $V_a = V_b$ and this is achieved through proper biasing of the transistor difference amplifier (consisting of two BC 147A transistors) following the differential input operational amplifier (op amp) stage. A dc power amplifier consisting of a driver transistor (SL 100) and a power transistor (2N 3055) makes the amplifier capable of driving the bridge with necessary amount of power, even when the FSH is immersed in water. The amplifier gains are kept at such a level that the stability of the controller is ensured while enough sensitivity is retained at the same time.

An analysis of the circuit relevant to this experiment is presented here with two fold objectives, namely

i) To obtain an expression for the transient power input to the FSH in terms of some accurately measurable variable.

ii) To identify a variable for providing an indication for the transient change in temperature δT. This is

necessary to ensure, on the basis of experimental data, that δT is indeed negligible.

2.5 Analysis of the electronic circuit

(A) An expression for power input interms of a measurable variable:

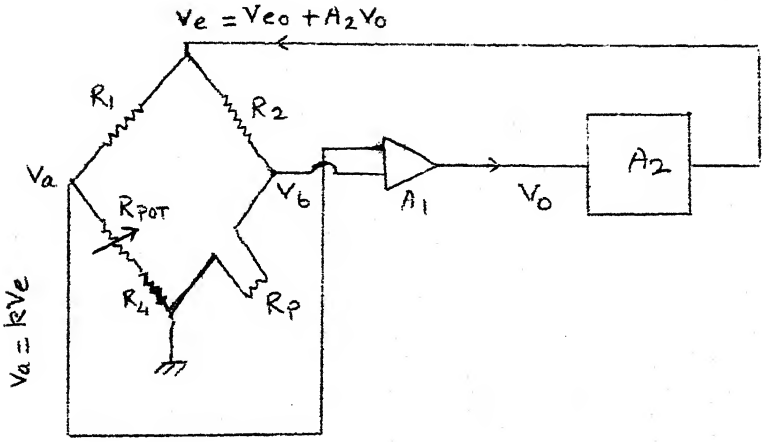

Fig. 2.5. Block diagram of controller circuit

Consider the block diagram of the circuit shown in figure 2.5.

At any time, the op amp output voltage, V_o, may be represented by the equation:

$$V_o = A_1 (V_b - V_a) \qquad (2.5 - 1)$$

and the bridge excitation voltage, V_e, by the equation:

$$V_e = V_{eo} + A_2 V_o \qquad (2.5 - 2)$$

where

V_a, V_b = bridge output voltages

A_1 = voltage gain of the op amp stage

A_2 = voltage gain of the differential amplifier stage

V_{eo} = bridge excitation voltage under steady state condition with $V_a = V_b$ and hence $V_o = 0$

As R_1, R_2 are fixed resistances and R_s ($= R_{POT} + R_4$) is fixed for a given setting of temperature, V_a can be expressed as a fraction of V_e by the expression :

$$V_a = kV_e \qquad (2.5\text{-}3)$$

where k is a constant chosen on the basis of bridge sensitivity consideration. (A typical value of k is 0.5)

Elemination of V_a from equations 2.5-1 and 2.5-3 gives:

$$V_b = \left(kV_e + \frac{V_o}{A_1} \right) \qquad (2.5\text{-}4)$$

If R_2 is the resistance in series with the FSH, then, power drawn, P_e, by the FSH is:

$$P_e = \frac{(V_e - V_b)}{R_2} \cdot V_b$$

Substitution of the value of V_b from equation 2.5-4 in the

above expression of P_e and subsequent rearrangement yields:

$$P_e = \frac{k(1-k)\, V_e^2}{R_2} - \frac{k(1-k)\, V_e\, V_o}{A_1\, R_2} - \frac{V_o^2}{A_1 R_2} \qquad (2.5\text{-}5)$$

Since $\left| \frac{V_o}{A_1} \right| \ll 1$, equation 2.5-5 may be approximated as:

$$P_e \simeq \frac{k(1-k)\, V_e^2}{R_2} \qquad (2.5\text{-}6)$$

Substitution for V_e from equation 2.5-2 in equation 2.5-6 leads to :

$$P_e = \frac{k(1-k)}{R_2} (V_{eo} + A_2 V_o)^2 \qquad (2.5\text{-}7)$$

Neglecting the higher order terms in equation 2.5-7 and on rearranging an expression of the following form is obtained:

$$P_e = \left(\frac{2A_2\, V_{eo} k^2}{R_p} \right) V_o + P_{eo} \qquad (2.5\text{-}8)$$

where $P_{eo} = \frac{k(1-k)}{R_2} V_{eo}^2$ i.e. the steady state power input to the FSH,

and R_p = resistance of the FSH at steady state.

Thus, we are able to express the transient power input interms of output voltage from the op amp stage which can be measured accurately. The advantage of measuring op amp output voltage is two fold :

a) The number of measurable variables reduces to a single one, as the transient power input which we are interested in, can be expressed in terms of op amp output voltage V_o.

b) The maximum sensitivity of the measuring instrument can be exploited as V_o starts from zero.

The power input P_e, as can be seen from the equation 2.5-8, is a linear function of V_o and hence a plot for calibration of power against V_o was prepared. The calibration procedure is described in section 2.6 and the results are presented in Chapter 3.

(B) Identification of a variable for the temperature change indication:

Under steady state condition with $V_a = V_b$ and hence $V_o = 0$ the bridge would be balanced.

Therefore, $V_e = V_{eo}$

and $$\frac{R_p}{R_2 + R_p} = k \qquad (2.5 - 9)$$

If the FSH resistance changes by a small amount δR_p due to temperature drop of its surface during the transient period accompanied by a change in the bridge excitation voltage from V_{eo} to V_e, then V_o can be expressed as:

$$V_o = A_1 \left[\left(\frac{R_p - \delta R_p}{R_p + R_2 - \delta R_p} \right) V_e - kV_e \right] \qquad (2.5\text{-}10)$$

Substitution of k from equation 2.5-9 in equation 2.5-10 gives

$$V_o = A_1 \left[\left(\frac{R_p - \delta R_p}{R_2+R_p-\delta R_p} \right) V_e - \frac{R_2}{R_2+R_p} V_e \right]$$

$$= A_1 \left[\frac{-R_2 \ \delta R_p}{(R_2 + R_p - \delta R_p)(R_2+R_p)} \right] V_e \qquad (2.5\text{-}11)$$

since $\delta R_p \ll R_2+R_p$; equation 2.5-11 can be simplified as:

$$V_o = - A_1 \ \frac{R_2}{R_p} \frac{\delta R_p}{R_p} \left(\frac{R_p}{R_2+R_p} \right)^2 \cdot V_e$$

Making use of equation 2.5-9 the above expression can be written as

$$V_o = - A_1(1-k) \ k^2 \ V_e \ \frac{\delta R_p}{R_p}$$

As $\frac{\delta R_p}{R_p}$ is proportional to δT for a FSH;

$$V_o = - A_1(1-k) \ k^2 \ V_e \ \delta T$$

Thus, a voltage change proportional to a change in temperature δT is obtainable at the output of the op amp stage. Strictly speaking V_o is not exactly proportional to δT because of the dependence of V_e on V_o as given in equation 2.5-2. However, if $V_o \ll V_{eo}/A_2$; then V_o is proportional to δT to a reasonable degree of approximation. This approach is justified because the ultimate use of the transient V_o produced due to a cooling

of the FSH is to establish the original premise that the FSH is being maintained at a constant mean temperature by negative feedback.

To verify that the change in the FSH temperature δT is indeed negligible in comparison to the temperature gradient, ΔT, responsible for heat transfer, one would simply have to measure V_o with the feedback removed. In the preliminary stage of this experiment this was done merely by changing the position of the switch S_1 to position 2 (figure 2.4) so that $V_e = V_{eo}$ and visually noting the responses in an oscilloscope.

2.6 Calibration procedure

The circuit was connected to a regulated dc power supply, a tecktronix 547 oscilloscope and a HP data acquisition system as shown in figure 2.4. The power supply was switched on and its voltage was slowly raised to 15V. The op amp output voltage was continuously monitored with the oscilloscope. With the heating of the FSH the oscilloscope beam started shifting from its initial zero setting. When the heater attained a steady state (within a few minutes) the bridge was balanced (i.e. oscilloscope reading was brought to zero setting) by adjusting the terturn potentiometer (R_{POT} in figure 2.4) of the bridge. Under this condition, the feedback loop was closed by changing

the position of the switch S_1 to 1 (figure 2.4).

In the closed loop condition, the steady state values of V_o, V_e, V_a, V_b and $V_e - V_b$ were measured with the data acquisition system. Once these values were obtained, slight unbalance in the bridge was created by adjusting the bridge potentiometer (R_{POT}) and steady state was again allowed to be reached. The feed back loop being closed, the bridge balance was restored quickly. However, in accordance with the proportional controller characteristic, V_o was different from zero due to this adjustment even after the attainment of steady state (off-set). At this stage the values of V_o, V_e, V_a, V_b and $V_e - V_b$ were again measured. This procedure was repeated for different R_{POT} settings and for each setting the steady state values of V_o, V_e, V_a, V_b and $V_e - V_b$ were measured. One set of reading is tabulated in table 3.1. Power was computed from equation 2.5-6 for different V_o values. The least square fit of power vs V_o is shown in figure 3.1. The experimental points are also shown on the same figure. The validity of this plot was verified both in air and water.

2.7 Fabrication of thermocouple embedded particle

The particle convective term Q_p was measured by means of a specially prepared moving cu-constantan thermocouple attached

to a copper bead. The copper bead served the purpose of a particle for disturbing the thermal boundary layer near the FSH and a thermocouple junction as well.

The first phase of preperation of thermocouple junction was the preperation of copper bead. As copper beads are not available they were prepared with the help of specially designed dies. Hammering technique was employed for preparing the copper beads of different sizes (0.25 mm., 0.35 mm, 0.65 mm). Surface irregularities were removed by rolling them in a small ball mill. After preparing the beads a through-and-through hole was made in each bead using 0.69 mm drill-bit on a precision lathe.

The thermocouple junction was formed by loop connection of a copper and a constantan wire of a cu-constantan thermocouple wire pair (TT-T 30, 30 gage, Omega make) and then soldering it (with ordinary solder) as shown in figure 2.6-a and 2.6-b. The copper bead (0.35 mm) was then heated with soldering iron and in hot condition one end of the thermocouple wire (constantan) was inserted into the hole of the bead and it was pulled until the soldered junction was nearly in the centre of the bead (figure 2.6-c). When the bead was cooled the solder firmly held the bead and the thermocouple wires inside the hole of the bead. In this

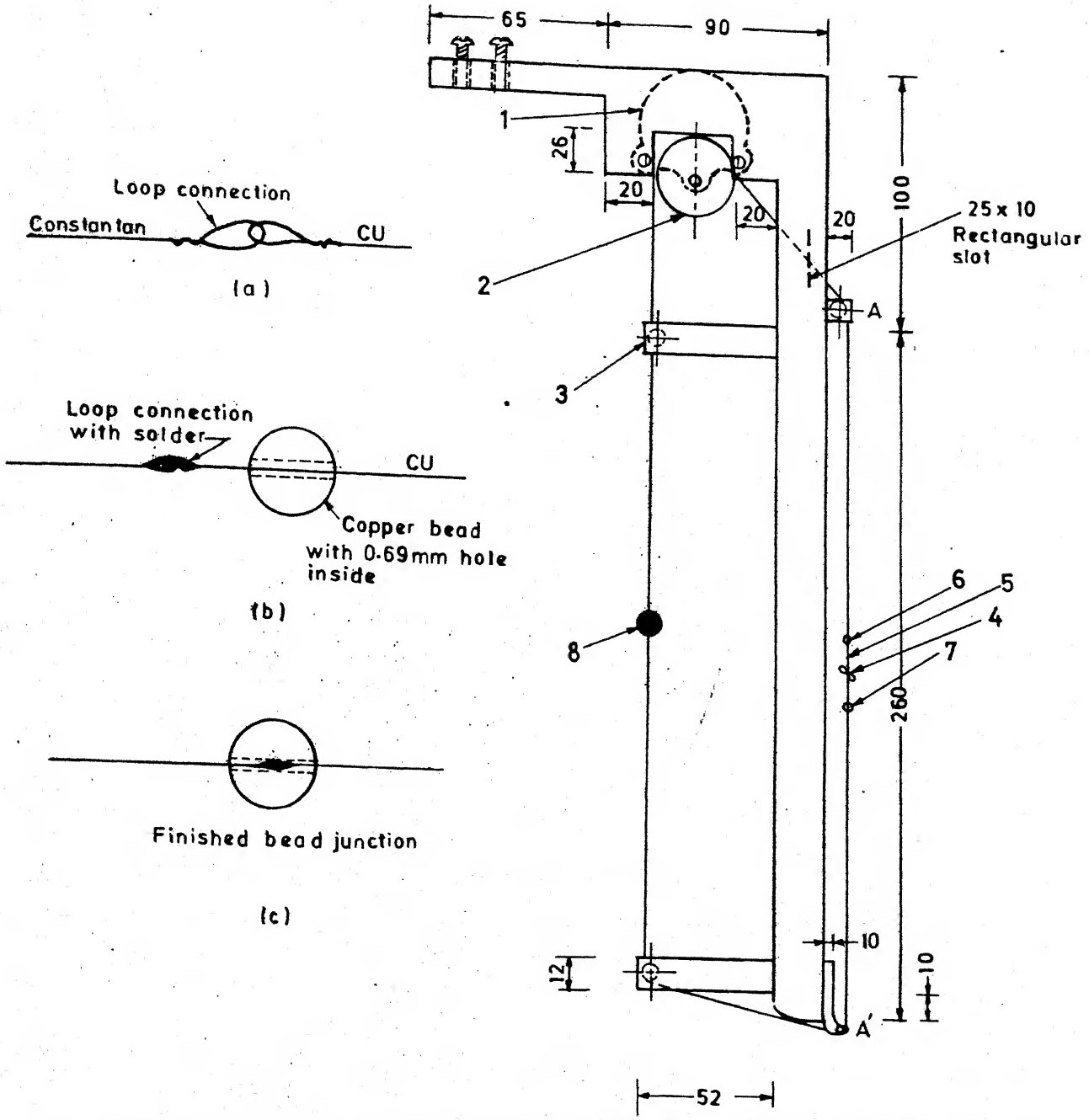

Fig. 2.6 Details of pully stand assemly and thermocouple junction (All dimension are in mm, not to the scale)

1) Synchronous motor
2) Pulley
3) Extended arm with small pulley
4) Knot
5) Plastic thread
6) Lead wire connection poi (cu-constantan junction as cold junction)
7) Lead wire connection point-2
8) Copper bead

process the copper bead itself was turned into a junction of the cu-constantan thermocouple. This junction was used as the hot junction. The thermocouple was then mounted on a removable pulley stand (material of construction was perspex) containing reversible synchronous motor as shown in figure 2.6-d. Other two ends of the thermocouple wires were connected to a plastic thread. The tension in the wires could be controlled by adjusting the knot of the plastic thread. Very fine and flexible copper wires were used as lead wires for this thermocouple. The thermocouple wire length and the lead wire connection points were so chosen that the cold junction never crossed the points A and A' shown in figure 2.6-d.

2.8 Experimental setup

The details of the experimental setup are shown in figure 2.7 and 2.8.

The flush mounted FSH was securely held inside a 5 litre beaker by means of clamps supported on stands (clamps and stands are not shown in figure). The details of connections are shown in figure 2.4 and 2.8.

The pulley stand assembly containing moving thermocouple was fitted on a removable X-Y bench which itself was screw

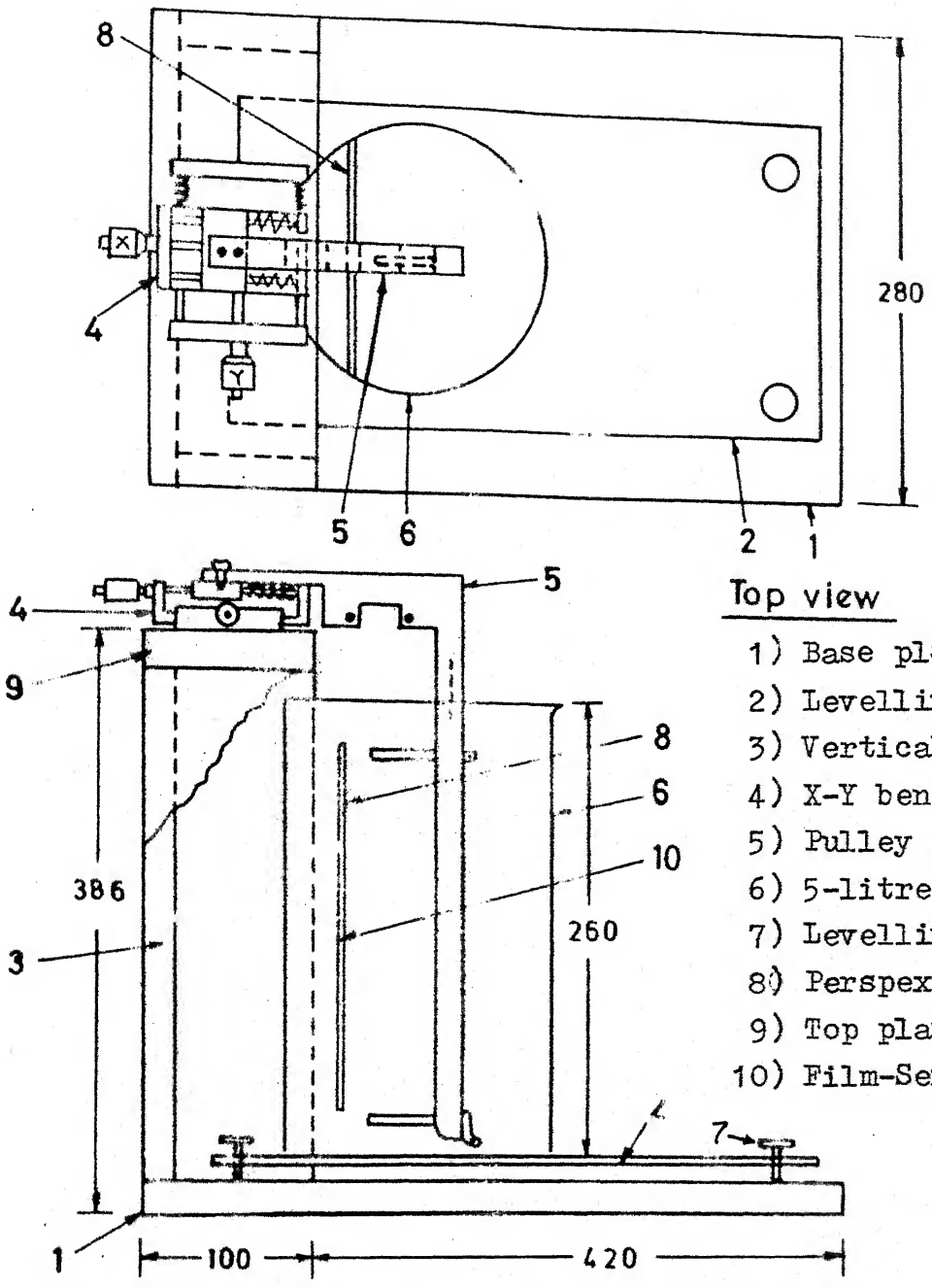

Fig. 2.7 Film sensor heater with pully stand assembly

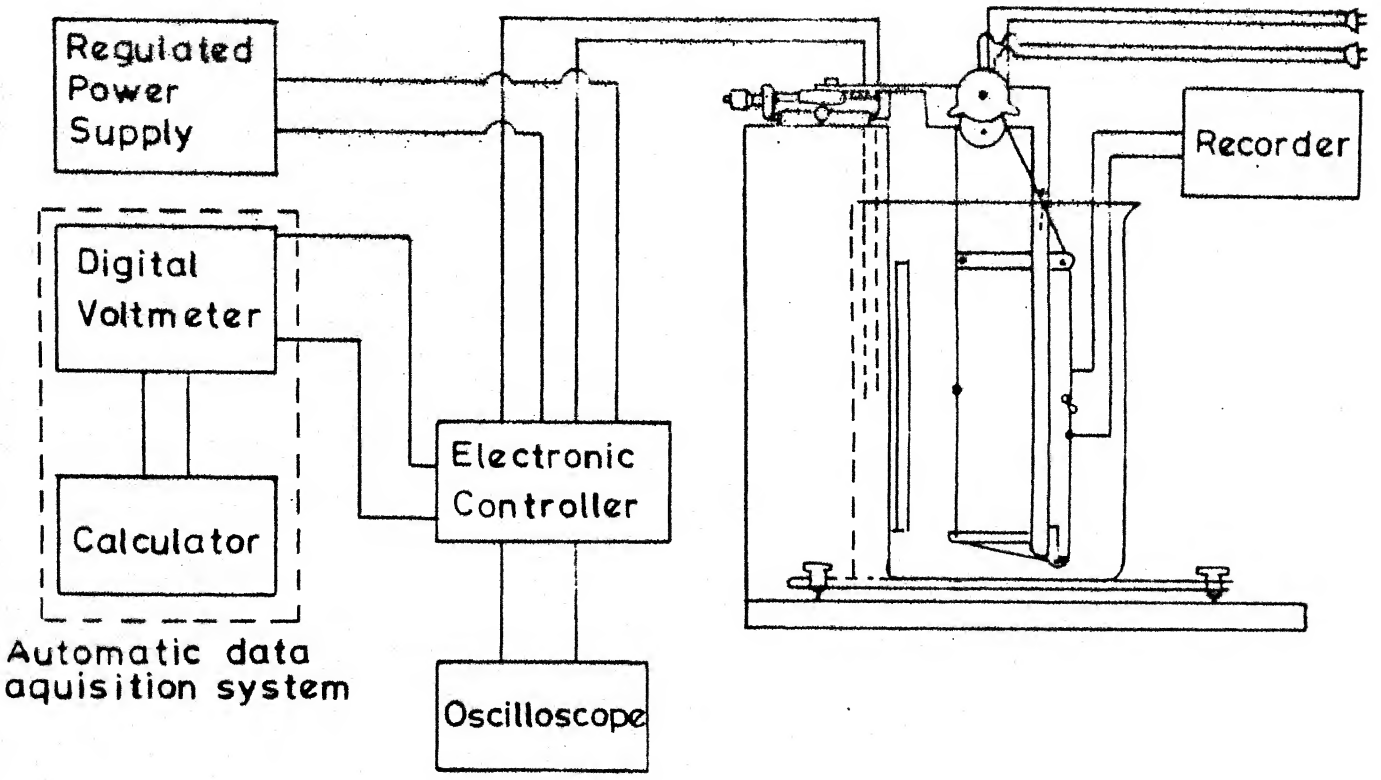

Fig.2.8 Schematic diagram of experimental set-up.

mounted on the support. The bead attached to the thermocouple could be positioned at any distance away from the wall by adjusting two micrometers of the X-Y bench and the distance between bead and the wall could be measured from the micrometer readings. The lead wires of the moving thermocouple were connected to an Omegaline strip chart recorder. All measuring instruments were properly grounded to keep the noise at a minimum level. Connections to the data acquisition system were made with low noise shielded wires.

2.9 Experimental Procedure

Initially the bridge was balanced as described in calibration procedure in section 2.6. After the steady state was attained the data acquisition system and the strip chart recorder was turned on. The copper bead (hot junction) was brought in front of the hot FSH by turning on the synchronous motor and then turning it off when the bead reached the centre line of the FSH. The bead was slowly brought near the centre of the heater surface by adjusting the micrometers of the X-Y bench. As soon as the bead touched the heater surface an abrupt change in the oscilloscope display was observed. When the bead made a contact with the FSH the

micrometer reading was taken to be zero. Then the X micrometer was readjusted to set the desired bead to wall (FSH) distance. Once the distance adjustment was over the motor was turned on and the ball was brought to the bottom position of the perspex wall where the temperature was equal to the bulk fluid temperature. The whole setup was then allowed to be reached the steady state (checked from recorder response and oscilloscope)

The recorder pen was adjusted to a chosen zero setting and it was switched on along with the reversible synchronous motor of the moving thermocouple assembly. During its vertically upward sweep, as soon as the copper bead crossed a predetermined mark on the perspex wall the digital voltmeter (DVM) of the data acquisition system was triggered on for taking transient readings at its maximum sampling rate of 20 readings per second.

The motor was switched off after the copper bead reached the upper predetermined mark on the perspex wall. The time required for the bead to cross these two predetermined marks on the wall was also noted by a stop-watch. This enabled us to calculate the velocity of the bead. The vertically upward motion was chosen to ensure that the initial bead temperature was same as the bulk fluid temperature.

From the output of the data acquisition system Q_t was calculated and from recorder reading Q_p was computed. Each set of experiments was repeated twice. Experiments were performed using one size of copper bead (0.35 mm.) and at one steady temperature level of the FSH but at different distances from wall (FSH) in air and water as well. As the purity of the water was found to affect the experimental runs (short-circuiting thermocouple wire and FSH contact points) extra pure deionised water (resistance 10^6 ohms) was used. A little oscillatory response was observed in water, hence average of the two readings were taken for water. All results are presented in Chapter 3.

CHAPTER - 3

RESULTS AND DISCUSSION

3.1 Additional power input due to particle motion

The transient output voltages of the op amp at different particle to wall (FSH) distances are presented in table 3.2 and table 3.3 for air and water respectively. Two typical results for air and water medium are also presented in the graphical form in figure 3.2 and figure 3.3 in which the point when the bead just came in front of the heater (entry point) and the point when it just crossed the heater (exit point) are shown.

A notable difference between the curves of the two systems is that the op amp output voltage V_o continues to increase in the negative direction even after the exit point and reaches a maxima. In contrast to this, in air medium V_o starts to decrease (in the negative direction) just after the exit point. As V_o is a measure of power input to the FSH it may be stated that power input continued to increase in water even after the exit point to reach a maxima while it decreased immediately after the exit point in air medium.

(All channel readings are in volts)

$V_e - V_b$	V_a	V_b	V_e	V_o
3.432650	3.166540	3.166105	6.605955	-0.248×10^{-3}
3.547345	3.271290	3.264795	6.790410	-9.665×10^{-3}
3.491355	3.229670	3.229320	6.727585	-6.542×10^{-3}
3.489255	3.227055	3.227400	6.724725	-6.579×10^{-3}
3.434625	3.172285	3.173500	6.614040	-0.61×10^{-3}
3.469885	3.201310	3.202365	6.672030	-3.319×10^{-3}
3.457465	3.194360	3.194395	6.660180	-2.784×10^{-3}
3.574095	3.294630	3.284105	6.826185	-11.164×10^{-3}
3.655025	3.382600	3.374110	6.997195	-21.225×10^{-3}
3.548970	3.298705	3.302025	6.873600	-15.106×10^{-3}
3.777330	3.346880	3.334500	7.044042	-24.648×10^{-3}
3.804330	3.371230	3.358890	7.094920	-27.408×10^{-3}
3.893950	3.466340	3.453300	7.277820	-38.065×10^{-3}
3.915590	3.467580	3.456680	7.297300	-38.844×10^{-3}
3.967790	3.531790	3.518260	7.412950	-45.824×10^{-3}

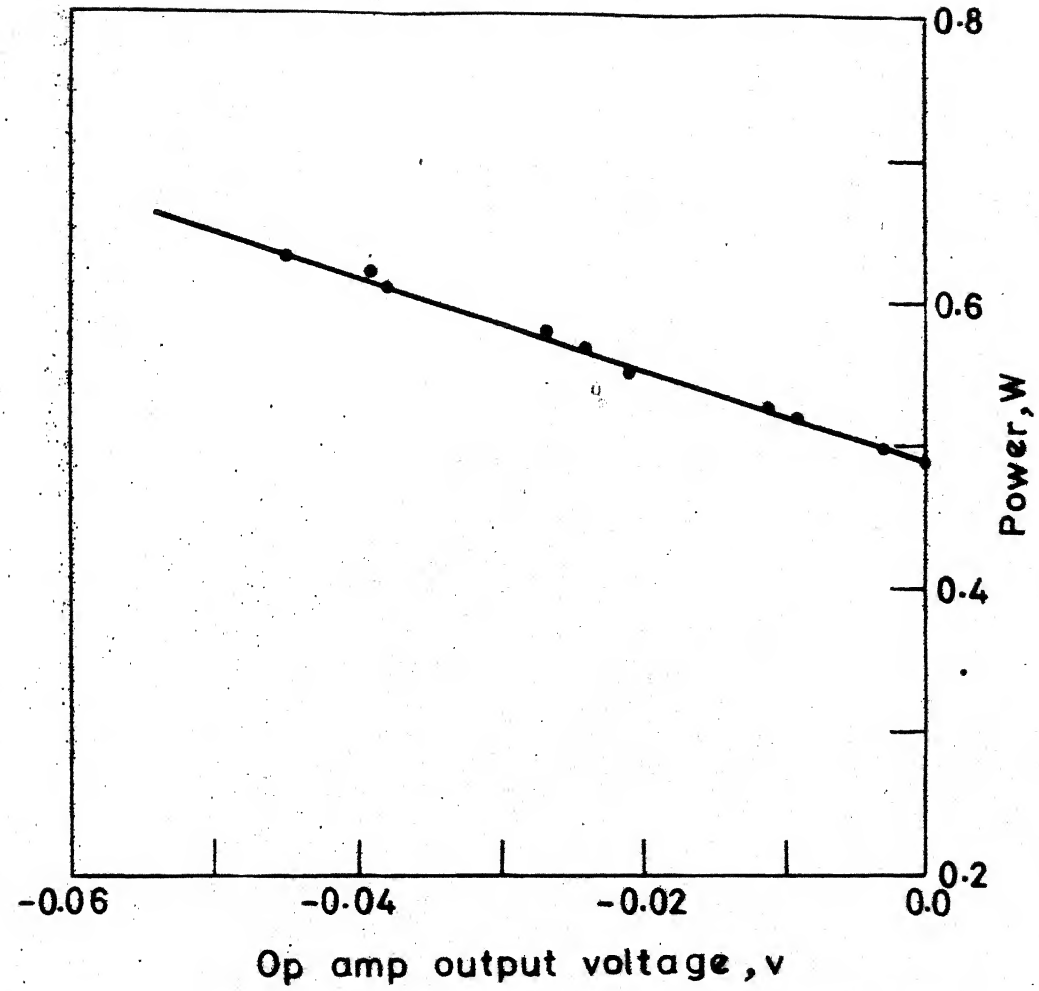

Fig. 3.1 Voltage-power calibration curve for film-sensor-heater

TABLE 3.2

Experimental data for transient output voltage of op amp.

(Op amp output in volts for various particle distances from wall)

System: Air [Average of two runs]

Time in sec. \ Distance	1.25 mm.	0.75 mm.	0.5 mm.	0.125 mm.	0.05 mm.
0.05	- 0.00063	- 0.00073	- 0.00096	- 0.00106	- 0.00136
0.01	- 0.00077	- 0.00115	- 0.00136	- 0.00204	- 0.00238
0.15	- 0.00102	- 0.00238	- 0.00315	- 0.00461	- 0.00525
0.20	- 0.00150	- 0.00337	- 0.00525	- 0.00837	- 0.01251
0.25	- 0.00205	- 0.00363	- 0.00637	- 0.00886	- 0.01604
0.30	- 0.00198	- 0.00349	- 0.00596	- 0.00822	- 0.01337
0.35	- 0.00187	- 0.00315	- 0.00549	- 0.00713	- 0.01040
0.40	- 0.00180	- 0.00288	- 0.00446	- 0.00641	- 0.00847
0.45	- 0.00156	- 0.00234	- 0.00299	- 0.00501	- 0.00555
0.50	- 0.00125	- 0.00175	- 0.00174	- 0.00352	- 0.00316
0.55	- 0.00084	- 0.00107	- 0.00111	- 0.00226	- 0.00181
0.60	- 0.00053	- 0.00061	- 0.00080	- 0.00155	- 0.00143
0.65	- 0.00034	- 0.00059	- 0.00071	- 0.00136	- 0.00100
0.70	-	- 0.00053	- 0.00064	- 0.00127	- 0.00093
0.75	-	-	- 0.00054	- 0.00115	- 0.00081
0.80	-	-	- 0.00049	- 0.00104	- 0.00079
0.85	-	-	-	- 0.00099	- 0.00069
0.90	-	-	-	- 0.00074	- 0.00065
0.95	-	-	-	- 0.00067	- 0.00056
1.00	-	-	-	- 0.00053	- 0.00044

- implies insignificant.

TABLE 3.3

Experimental data for transient output voltages of Op amp.

(Op amp output in volts for various particle distances from wall)
[Average of two runs]

System : Water

Time in seconds	Distances 1 mm.	0.50 mm.	0.25 mm.	0.15 mm.
0.5	- 0.0030	- 0.0046	- 0.0065	- 0.0200
1.0	- 0.0140	- 0.0160	- 0.0195	- 0.0298
1.5	- 0.0190	- 0.0220	- 0.0250	- 0.0290
2.0	- 0.0200	- 0.0210	- 0.0240	- 0.0280
2.5	- 0.0270	- 0.0200	- 0.0230	- 0.0250
3.0	- 0.0150	- 0.0180	- 0.0210	- 0.0228
3.5	- 0.0140	- 0.0160	- 0.0200	- 0.0215
4.0	- 0.0130	- 0.0150	- 0.0185	- 0.0210
4.5	- 0.0125	- 0.0142	- 0.0170	- 0.0195
5.0	- 0.0120	- 0.0130	- 0.0160	- 0.0190
5.5	- 0.0100	- 0.0115	- 0.0145	- 0.0178
6.0	- 0.0085	- 0.0090	- 0.0130	- 0.0165

P.T.O.

Table 3.3 Continued.

Time in seconds	Distances 1 mm.	0.50 mm.	0.25 mm.	0.15 mm.
7.0	- 0.0070	- 0.0085	- 0.0120	- 0.0159
8.0	- 0.0050	- 0.0070	- 0.0098	- 0.0142
9.0	- 0.0030	- 0.0050	- 0.0072	- 0.0110
10.0	- 0.0020	- 0.0035	- 0.0060	- 0.0100
11.0	- 0.0010	- 0.0027	- 0.0045	- 0.0080
12.0	-	- 0.0013	- 0.0030	- 0.0068
13.0	-	- 0.0010	- 0.0015	- 0.0050
14.0	-	-	- 0.0012	- 0.0036
15.0	-	-	- 0.0090	- 0.0027
16.0	-	-	-	- 0.0018
17.0	-	-	-	- 0.0012
18.0	-	-	-	- 0.0010

- implies insignificant

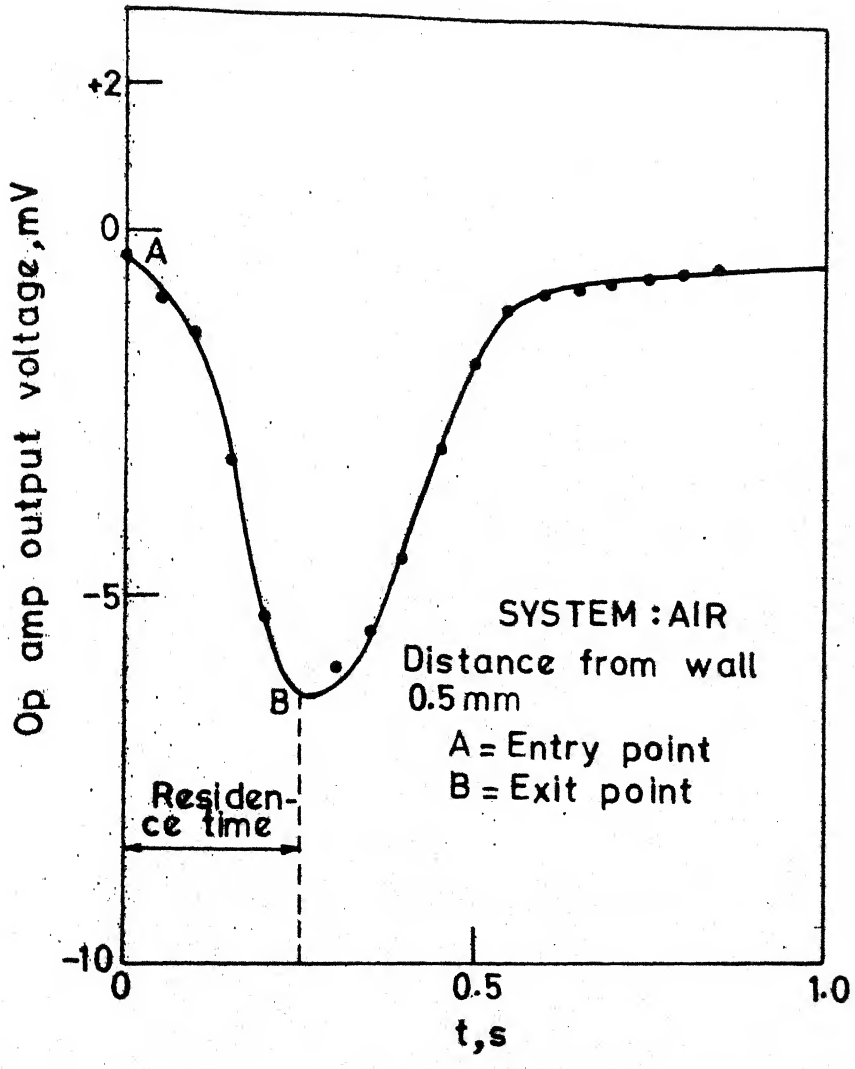

Fig. 3.2 Variation of op amp output voltage with time due to particle movement in air.

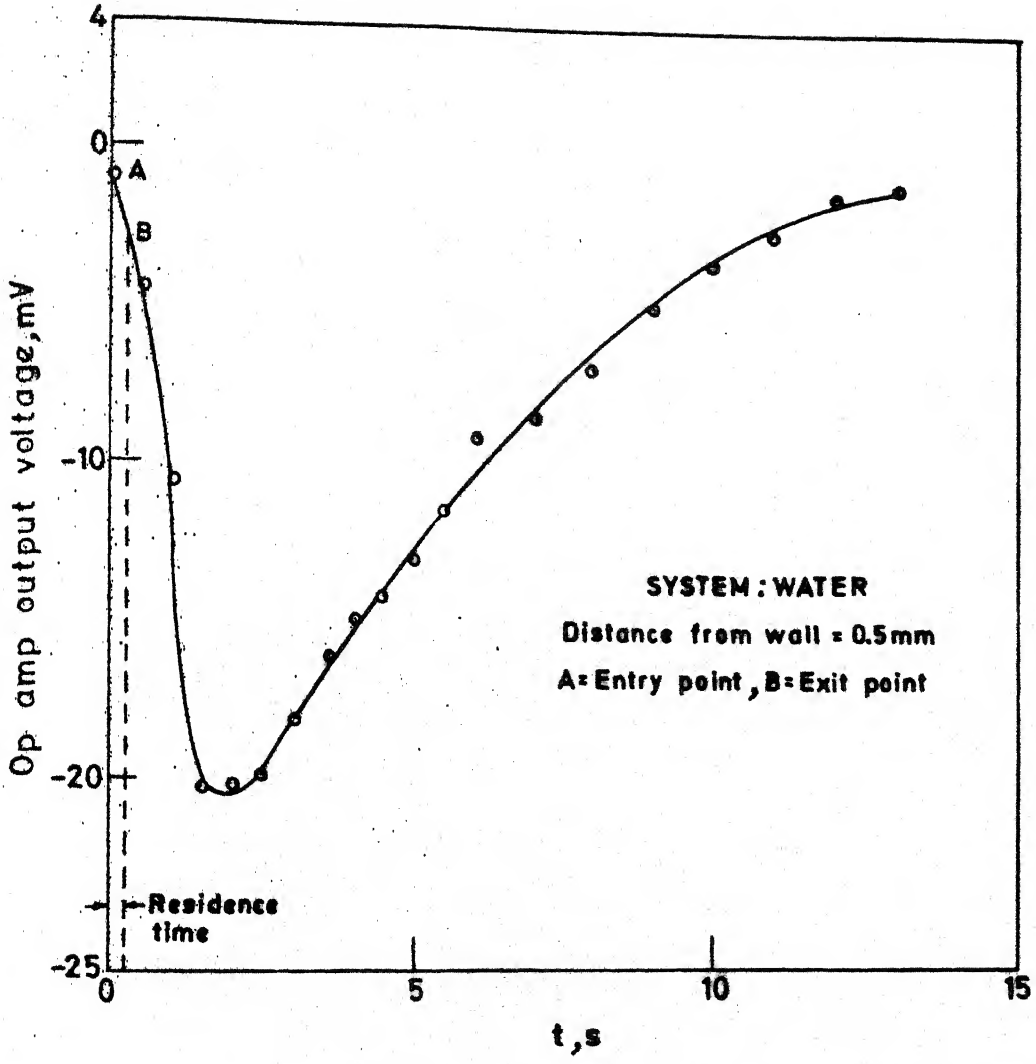

Fig. 3.3 Variation of op amp output voltage with time due to particle movement in water

The increase in power after the exit point in water medium was due to the inertial effect of water. Water being many times denser than air, the fluid drift behind the particle brought in larger amount of cold water from bulk compared to air which continued to take appreciable amount of energy away from the heater surface and hence the increase in power.

The additional power input to the FSH was computed from the calibration chart given in figure 3.1. The variation of additional power input with time as a function of particle to wall (FSH) distance are shown in figure 3.4 and figure 3.5 for air and water respectively.

As the volumetric heat capacity of water is large compared to air, heat removal from or near the heater surface is more in water even though the temperature difference between the heater and bulk fluid is higher in air. As it needs more power input to keep the FSH at constant temperatur the peak value of the power-time curve in water is always higher than that in air.

The enhanced heat transfer term Q_t due to particle motion was computed from the area under the curves shown in figure 3.4 and figure 3.5 for air and water mediums.

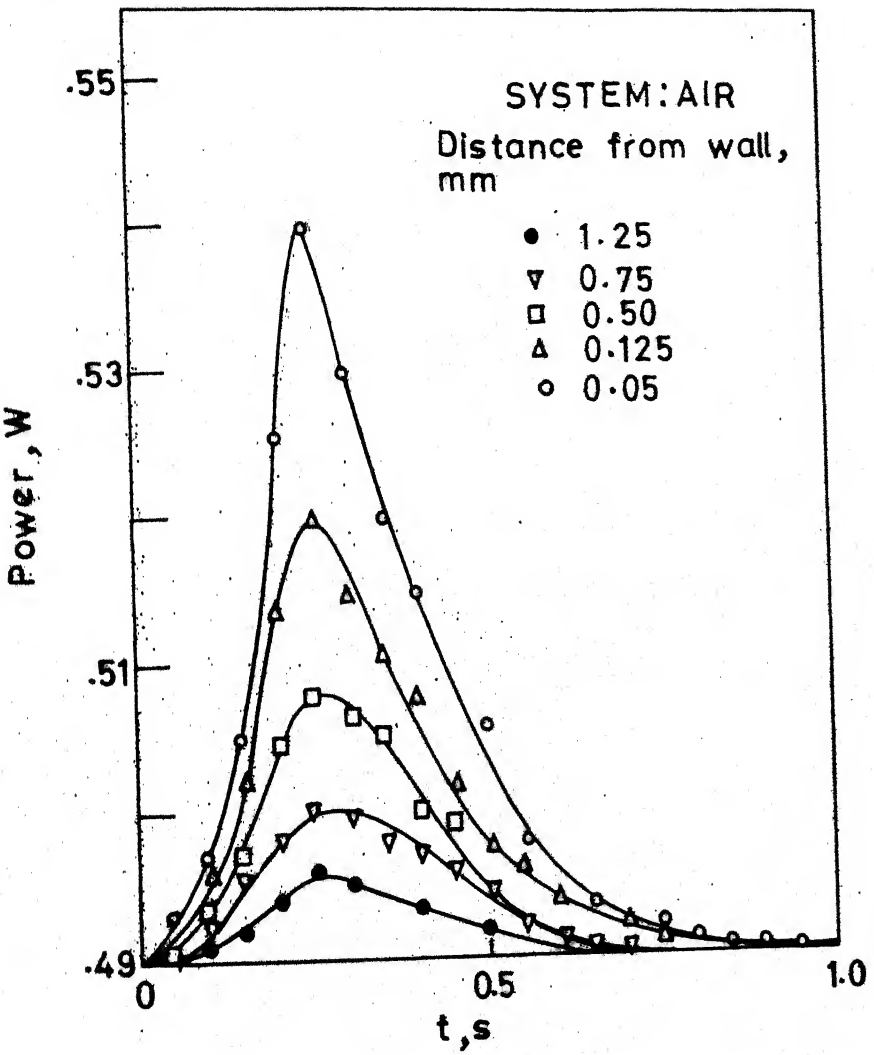

Fig. 3.4 Additional power input with time due to particle movement in air

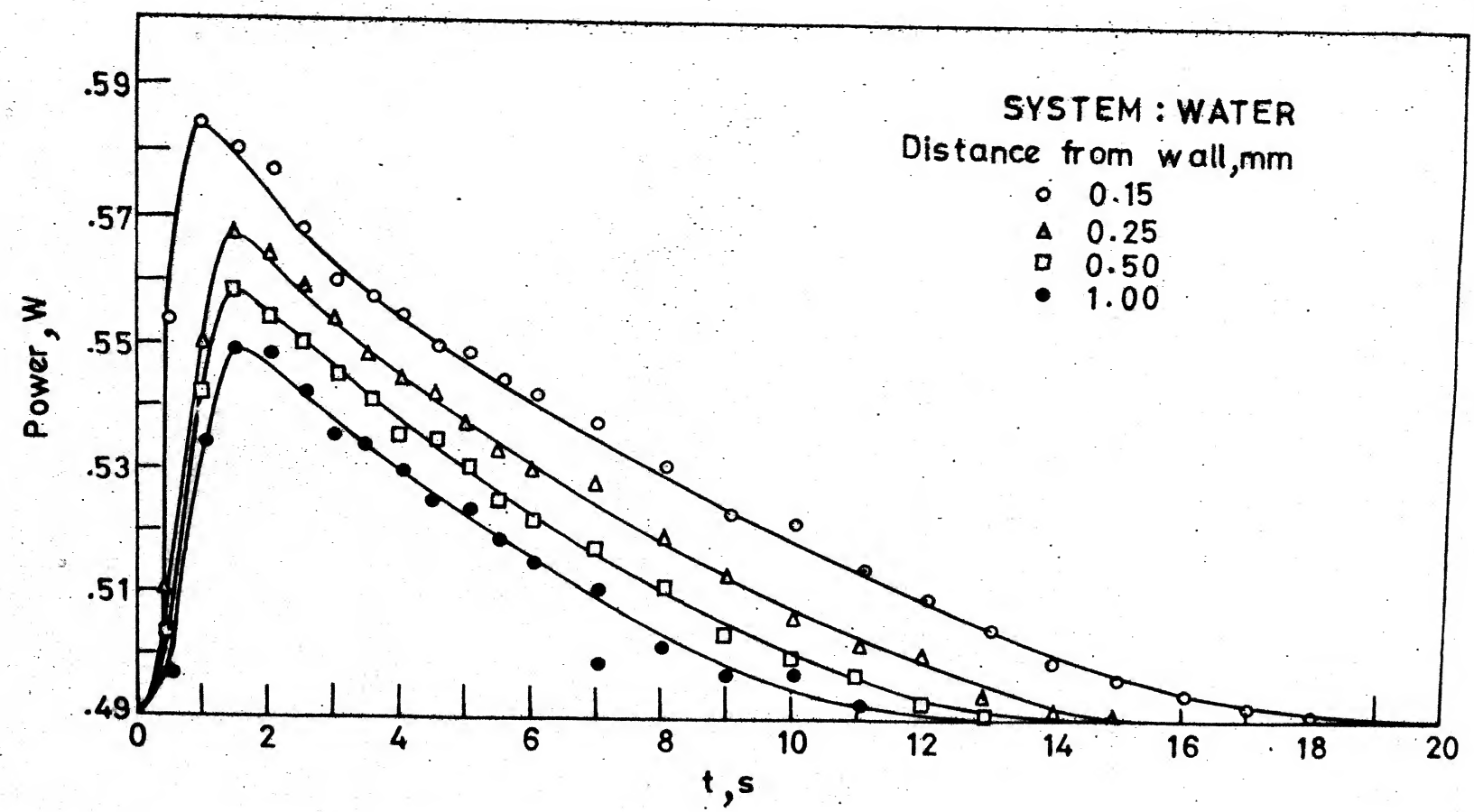

Fig. 3.5 Additional power input with time due to particle movement in water

3.2 Energy picked up by the particle, Q_p

The energy picked up by the particle (Q_p) as it sweeped past the heater surface was computed from the strip chart recorder trace. The standard emf to temperature conversion table for the cu-constantan thermocouple was used for computation of temperature from the trace and the copper bead was assumed to be at uniform temperature throughout (i.e. no temperature gradient within the bead). The justification of this assumption is given below:

Whenever a sphere, initially at a uniform temperature, is exposed to an isothermal fluid at a different temperature for a short period of time, the temperature at any radial position of the sphere can be computed from the well known Heisler charts [8]. For the copper bead (used in this study) the maximum Biot number in water medium is 1.3×10^{-2} (calculations are shown in appendix 1) and the temperature difference between the centre and the surface is negligible even at a Fourier number of 0.183 which is 1/50th of the time to cross over the hot surface. Hence the copper bead may be considered to be at a uniform temperature. In the actual situation, however, only a part of the bead surface is exposed to a hotter region and the other part to a colder region as shown in figure 3.2-1(a). In view of the

above discussion, even for this case it is considered that the temperature within the bead is uniform at any instant of time.

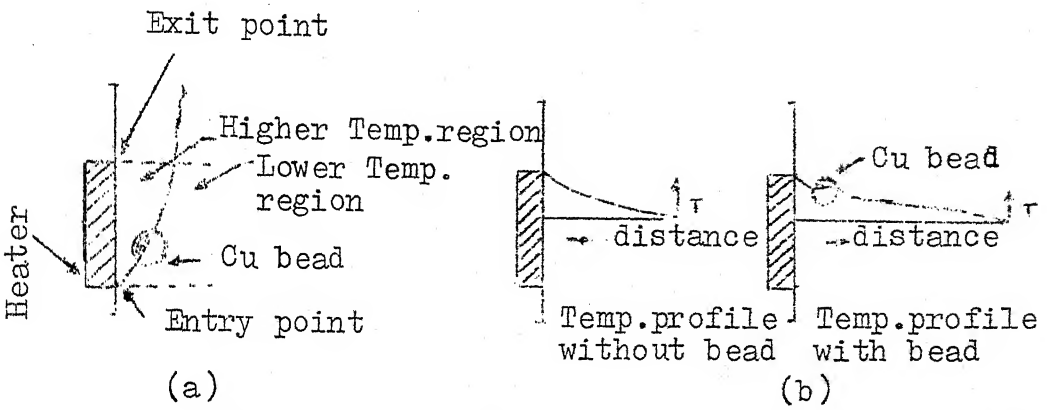

Fig. 3.2-1. Modification of temperature profile in presence of the particle.

Because the particle temperature is uniform, the temperature profile near wall gets modified as shown in figure 3.2-1(b). Thus the particle effectively decreases the heat transfer resistance. This mode of enhancement in heat transfer has been considered in modelling of heat transfer in fluidized beds [Saxena and Gabor (18)] and is referred to as conduct heat transfer. The contribution of this mode of heat transfe towards the total enhanced heat transfer in the time interva between entry and exit point of the particle (copper bead) infront of the heater surface is small in water but it could be significant in air. However, this mode of transfer is lumped with the fluid convective transfer and no attempt was made to separate it.

The computed Q_p values are tabulated in table 3.4 and two typical experimental recordings areshown in photograph 3P-1 & 3P-2.

The nature of the response of the thermocouple may be interpretated as follows:

As the copper bead entered the thermal boundary layer its temperature increased and the emf of the thermocouple increased. During its upward sweep more and more area of the bead got exposed to the thermal boundary layer which itself grew thicker from the point A onwards as shown in figure 3.2-1(a). In addition to that, the effect of natural convection became more and more prominent as the bead moved away from the heated surface during its upward journey. That was why temperature of the bead continued to rise even after it had crossed the FSH and finally reached a steady value. As the position at which the bead was stopped was not very far from the FSH the bead continued to be in the plume of rising hot fluid and hence it remained at a higher temperature level than that of the bulk fluid.

3.3 Evaluation of Q_{fc} and comparison of Q_{fc} and Q_p

The fluid convective transfer term, Q_{fc}, was computed from the difference between Q_t and Q_p (It may be pointed out

TABLE 3.4

Experimental data of thermocouple reading for computing Q_p

[Average of two runs]

System	Particle Distance from wall in mm.	Milli Volt reading in 10^{-3}	Temp. rise in 10^{-2} °C	Q_p milli Joules
	1.25	0.625	1.55	1.420
	0.75	1.25	3.11	2.390
Air	0.50	2.00	5.00	3.844
	0.125	4.00	10.00	7.678
	0.05	6.55	16.64	12.490
Water	1.00	0.80	2.00	1.54
	0.50	1.00	2.50	1.92
	0.25	3.00	7.50	5.76
	0.15	4.00	10.00	7.69

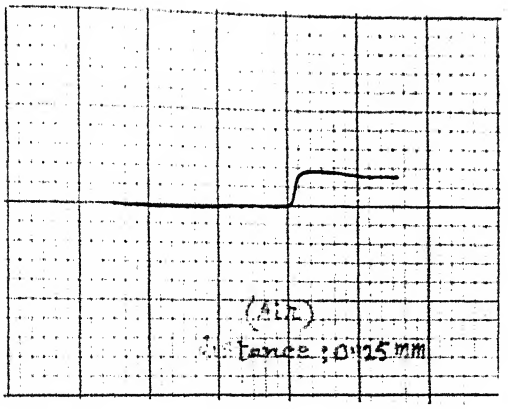

Photograph 3P-1. Thermocouple response in air

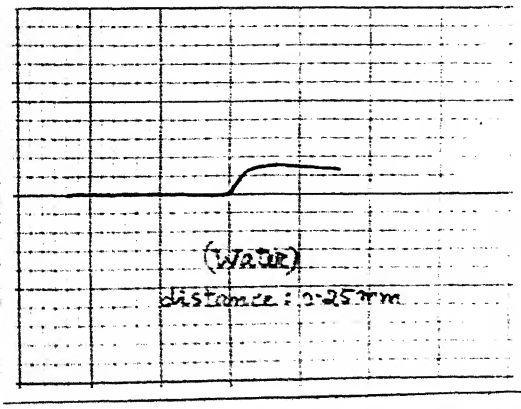

Photograph 3P-2. Thermocouple response in water

that the way Q_{fc} was calculated it included the conductive term as well). Figure 3.6 and figure 3.7 shows the variation of Q_t, Q_p and Q_{fc} with the particle distance from wall (FSH) for air and water respectively.

The relative contributions of Q_p and Q_{fc} toward Q_t are tabulated in table 3.5. As expected, the value of Q_p increased sharply as the distance between particle and the wall decreased. However, the fluid convective term increased rather gradually. It can be seen that beyond 1-1.5 particle diameter the particle will have no effect on the heat transfer from the wall. With decrease in distance between particle and wall both Q_p and Q_{fc} are expected to increase. The lower value of Q_{fc} observed in one reading (figure 3.6) may be attributed to the experimental error. As the film was susceptible to damage due to rubbing (by copper bead) such close distances were avoided in water where distance adjustment was difficult due to refractive index of water.

The final results show that the contribution of Q_p towards Q_t is higher (65-73%) in air while the contribution of Q_{fc} is almost 99% in water.

The findings are in accordance with the generally accepted views that the particle convective mechanism is dominent in air and fluid convective mechanism in water.

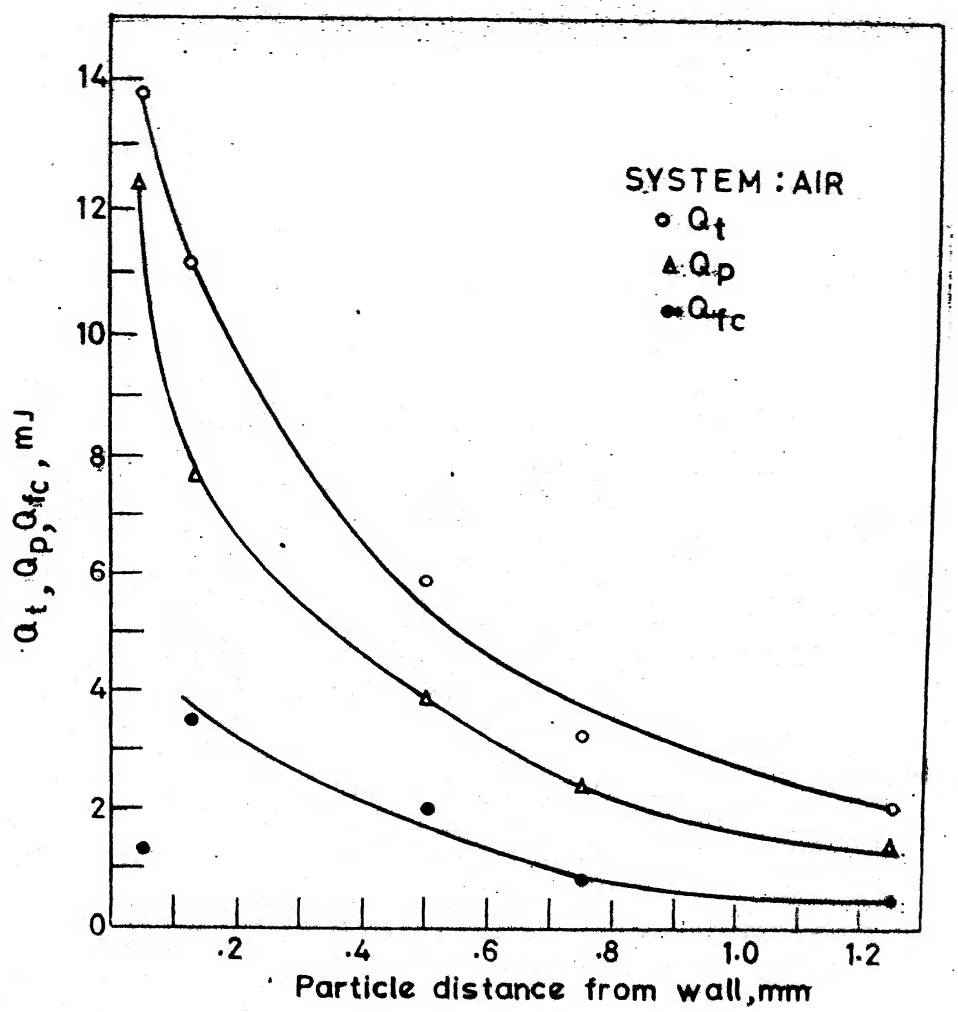

Fig. 3.6 Variation of Q_t, Q_p and Q_{fc} with distance in air

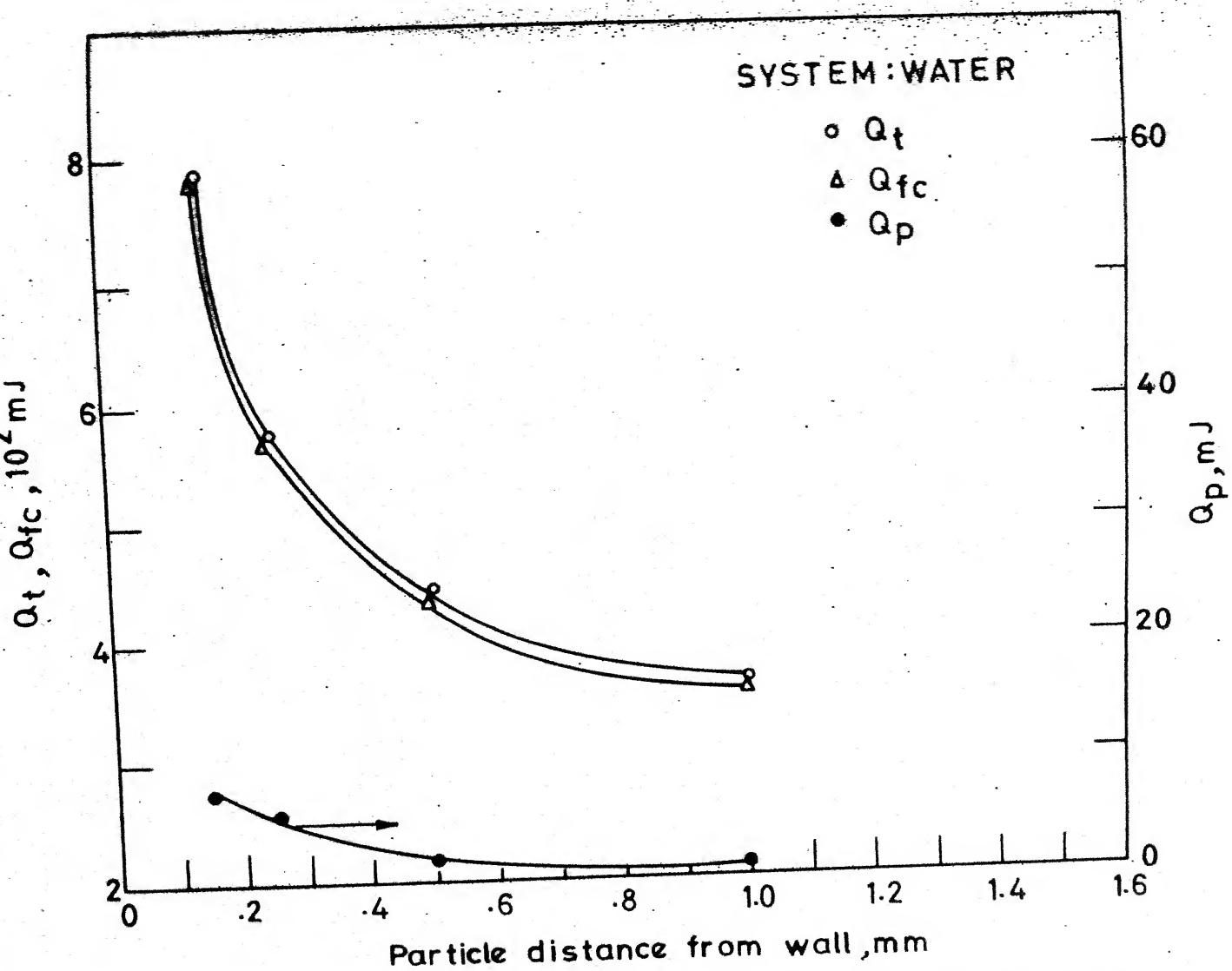

Fig. 3.7 Variation of Q_t, Q_p and Q_{fc} with distance in water

TABLE 3.5

Relative Contributions of Q_p and Q_{fc} toward Q_t

Q_t milli Joules	Q_p milli Joules	% contribution of Q_p	Q_{fc} milli Joules	% contribution of Q_{fc}
Air				
2×10^{-3}	1.42×10^{-3}	71%	0.58×10^{-3}	29%
3.25×10^{-3}	2.39×10^{-3}	73.5%	0.86×10^{-3}	26.5%
5.9×10^{-3}	3.844×10^{-3}	65%	2.056×10^{-3}	35%
11.2×10^{-3}	7.678×10^{-3}	68.5%	3.522×10^{-3}	31.5%
13.8×10^{-3}	12.49×10^{-3}	90%	1.31×10^{-3}	10%
Water				
3.75×10^{2}	1.54×10^{-3}	0.05%	3.73×10^{2}	99.5%
4.42×10^{2}	1.92×10^{-3}	0.05%	4.401×10^{2}	99.5%
5.775×10^{2}	5.76×10^{-3}	1%	5.7174×10^{2}	99%
7.8895×10^{2}	7.69×10^{-3}	1%	7.8126×10^{2}	99%

3.4 Heat transfer coefficient, conduction loss and percent improvement in heat transfer

To have an estimate of steady state heat transfer coefficient from the FSH to the fluid a knowledge of steady state conductive losses through the substrate is required. This in turn, again needs a knowledge of back surface temperature (glass surface temperature) of the FSH. However, back surface temperature could not be determined after mounting the FSH with quickfix. Instead, the correlations available in literature were used for computing heat transfer coefficient and steady state convective heat transfer from the hot film surface to surrounding fluid was computed from the following equation:

$$\dot{Q}_c(s) = h(s), A\ (T_f - T_b)$$

where $h(s)$ = average steady state heat transfer coefficient from the FSH to surrounding

A = area of the film

T_f = average film temperature

T_b = bulk fluid temperature.

The nature of the thermal boundary is such that the variation in temperature is likely to be minor in the vertical direction

The average film temperature was determined from the following relation [4] :

$$R_T = R_o [1 + \alpha_o (T - T_o)]$$

where T_o = reference temperature at which resistance is R_o

R = operating resistance

T = operating temperature

α_o = temperature coefficient of resistance at the reference temperature T_o

The following correlation for short vertical plates [15] was used for computing the heat transfer coefficients:

$$Nu = \left(\frac{Gr}{4}\right)^{1/4} \cdot \frac{0.902\ (Pr)^{1/2}}{(0.861 + Pr)^{1/4}}$$

where

Nu = Nusselt number

Pr = Prandtl number

Gr = Grashof number

Once $\dot{Q}_c(s)$ was known $Q_k(s)$ was computed from equation 2.1. These values are tabulated in table 3.6. The variations of heat transfer coefficient of the hot FSH (in this setup) with time due to particle movement are shown in figure 3.8 and 3.9 for air and water respectively. The transient heat transfer coefficient h(t) was calculated directly from the experimental data.

The percentage improvements in convective heat transfer from hot film due to particle movement were also computed at different particle to wall (FSH) distances both for air and water systems. These are tabulated in table 3.7 along with the particle Reynolds number for two systems.

TABLE 3.6

Estimated Conductive and Convective losses

System	Room Temperature °C	FSH Temperature °C	Steady state power input(W)	$\dot{Q}_k(s)$ (W)	$\dot{Q}_c(s)$ (W)
Air	17	65	0.49	0.4454	0.0446
Water	16	23	0.49	0.1669	0.3231

TABLE 3.7

Percent improvement in convective heat transfer

System	Particle distance from wall (mm)	$Q_c(s)$ (Joules)	Improved Q_c (Joules)	% Improvement
Air	1.25	0.0446 x 0.7 = 0.03122	2×10^{-3}	6.41
(Re= 4.18)	0.75	0.0446 x 0.75= 0.03345	3.25×10^{-3}	9.72
	0.50	0.0446 x 0.80= 0.03568	5.9×10^{-3}	16.54
	0.125	0.0446 x 0.90= 0.04014	11.2×10^{-3}	27.90
	0.05	0.0446 x 1.00= 0.04460	13.8×10^{-3}	30.94
Water	1.00	0.3231 x 12.5 = 4.03875	0.37500	9.29
(Re= 62.36)	0.50	0.3231 x 13.2 = 4.26492	0.44200	10.36
	0.25	0.3231 x 15.3 = 4.94343	0.57750	11.68
	0.15	0.3231 x 19 = 6.13890	0.78895	12.85

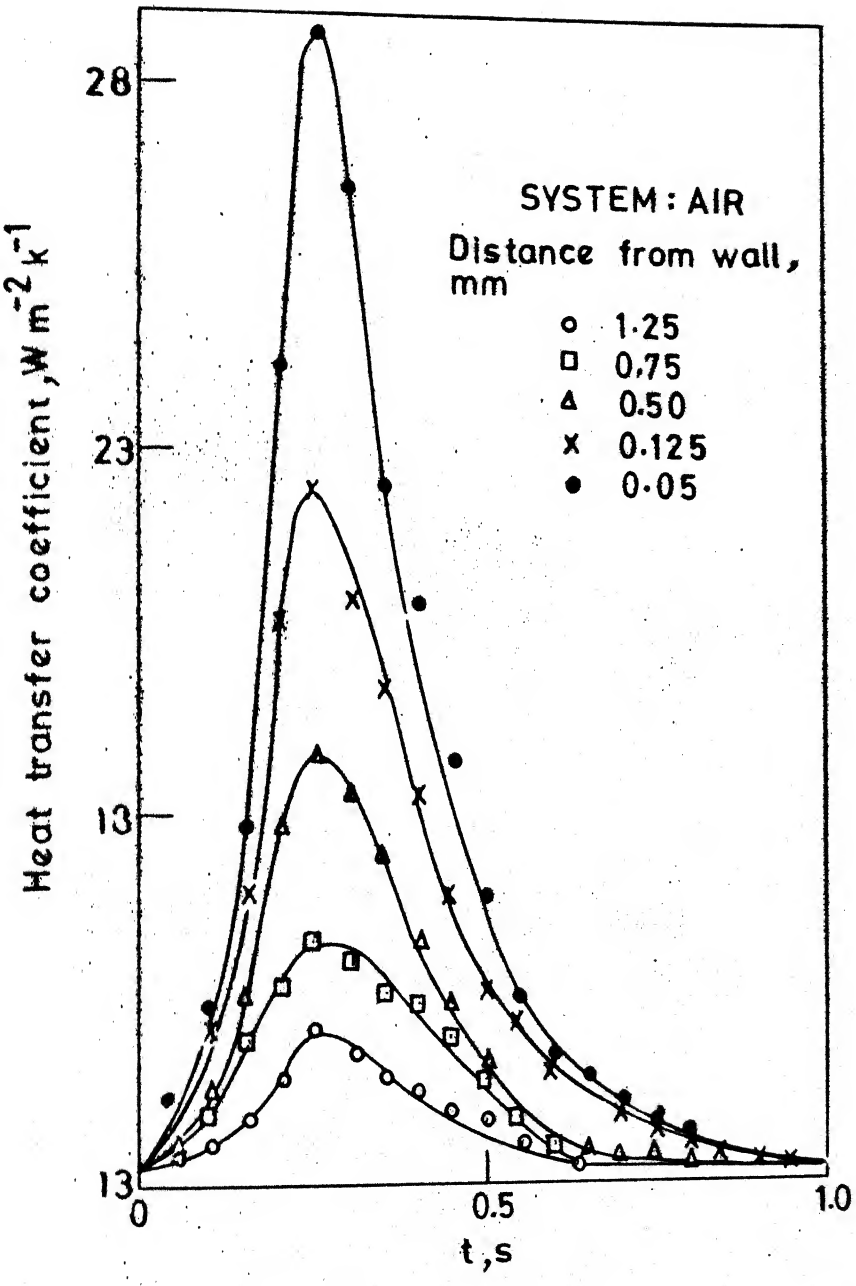

Fig. 3.8 Variation of average heat transfer coefficient with time due to particle movement in air

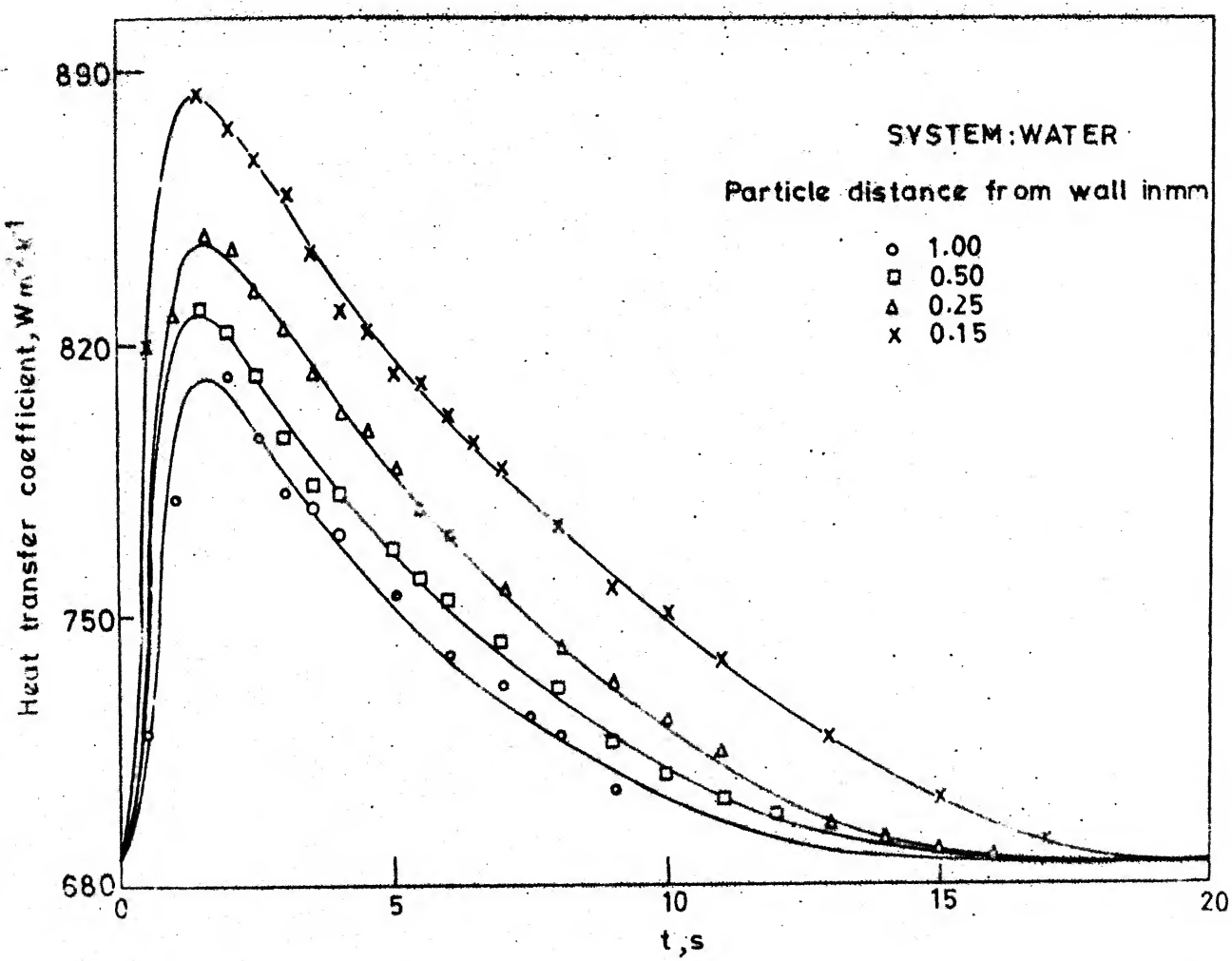

Fig 3.9 Variation of heat transfer coefficient with time due to particle movement in water

CHAPTER - 4

CONCLUSION AND SUGGESSIONS

4.1 Conclusion of the present work

A constant temperature film-sensor-heater and a mechanism for moving a particle with embedded thermocouple were developed. The enhencement in heat transfer, the nature of enhancement and the relative contributions of particle and fluid convective transfer terms toward the total transfer were studied in air and water for different particle to wall (transfer surface) distances. The particle convective transfer was found to be significant (65-73%) in air medium while the fluid convective transfer was found to be the sole (99%) mode of transfer in water medium.

The enhancement process continued quite for some time in water medium even after the particle had crossed over the transfer surface due to the inertial effect of water. In contrast to this, the enhancement in heat transfer rate in air medium ceased immediately after the particle had crossed over the transfer surface. Between the two systems air and water, enhancement process was always higher in air under the experimental conditions used in this work.

4.2 Suggessions for future work

To gain more insight into the mechanism of heat transfer and to obtain correlations for predicting heat transfer coefficients in fluidised beds extensive studies need to be conducted over wide range of variables like velocity, size and number of particles, particle to wall distances and film temperature.

Precise estimate of back surface temperature of the FSH should be made for computing steady state heat transfer coefficients from experimental data. The back temperature can be measured by coating platinum on the back side as well as measuring the resistance in the similar way as was done for the front side.

To simulate conditions similar to that in a fluidized bed developing boundary layer should be avoided and this can easily be achieved by arranging three heaters as shown in figure 4.2-1

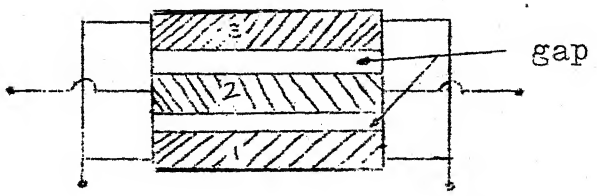

Fig. 4.2-1. Suggested heater assembly.

Only the second heater need to be kept at constant mean temperature by negative feedback control mechanism. The other two guard heaters (1 and 3) should only be used to form a continuous thermal boundary layer. A flat thermal boundary layer can be obtained by proper choice of the width of the guard heaters. Spherical particles with low thermal conductivity value (hence negligible Q_p) can also be used in the present setup for computing Q_{fc} directly from the FSH response.

As the platinum film is susceptible to damage during handling, a thin protective coating of MgF_2 or SiO_2 on the film is suggested. The FSH construction technique employed was tedeous and time consuming. Hence vapour deposition technique is suggested in the future work.

Although this constant temperature FSH was developed for heat transfer study it will also find its application in shock tubes, wall shear stress measurements, animometry and resistance thermometry.

REFERENCES

1. Adams, R.L. and Welty, J.R., AIChE J., 25, 395 (1979)
2. Baskakov, A.P. and Suprun, V.M., Int. Chem. Eng., 12, 324 (1972)
3. Botterill, J.S.M., " Fluid-Bed Heat Transfer ", Academic Press New York (1975)
4. Christensen, Orla, "New Trends in Hot-film Probe Manufacturing DISA Information No.9, Feb. 1970
5. Ganzha, V.L., Upadhyay, S.N. and Saxena, S.C., Int. J. Heat Mass Trans., 25 (10), 1531 (1982)
6. Gelprin, N.I. and Einstein, V.G., in "Fluidization", Edited by Davidson, J.F. and Harison, D., Academic Press, (1971).
7. Gutfinger, C. and Abuaf, N., Adv. Heat Transfer, Academic Press, Vol.10, 167 (1974)
8. Heisler, M.P., Trans. A.S.M.E., 69 , 227 (1947)
9. Kunii, D. and Levenspiel, "Fluidization Engineering", Wiley, New York (1969)
10. Leva, M., "Fluidization", McGraw-Hill, New York, (1959)
11. Ling, S.C., ASME J., Basic Engr, 82, 629 (1960)
12. Mickley, H.S. and Fairbanks, D.F., AIChE J. 1 , 374 (1955)
13. NASA CR-26 Contractor Report, April 1964
14. Rao, D.P., Ph.D. Thesis, BITS Pilani (1973)

15. Rosenhow, W.M. and Choi, H.Y., "Heat Mass and Momentum Transfer", Prentice-Hall, INC., New Jersey (1961)

16. Sandborn, V.A., "Resistance Temperature Transducers", Metrology Press, Fort Collins, Colorado (1972)

17. Saxena, S.C., Granal, N.S., Gabor, J.D., Zabrodsky, S.S. and Galershtein, D.M., Adv. Heat Transfer, Academic Press, Vol.14, 149 (1978)

18. Saxena, S.C. and Gabor, J.D., Prog. Eng. Combust. Sci., 7 , 73 (1981)

19. Subramanian, N., Rao, D.P. and Gopichand, T., Ind. Eng. Chem. Fund., 12(4), 479 (1973)

20. Verma, A.K., personal communication.

21. Washmund, B. and Smith, J.W., Can. J. Chem. Eng., 45, 156 (1967)

22. Zabrodsky, S.S., Epanov, Yu.G., Galershtein, D.M., Saxena, S.C. and Kolar, A.K., Int. J. Heat Mass Trans., 24(4) 571(198

23. Zabrodsky, S.S., "Hydrodynamics and Heat Transfer in fluidize beds", Engl. Transl. by Zenz, F.A., M.I.T. Press, Cambridge, Massachusetts, 1966.

24. Zenz, F.A. and Othmer, D.F., "Fluidization and Fluid Particle Systems", Rein hold, New York, 1960

25. Zeigler, E.N., Koppel, L.B., and Brazelton, W.T., Ind. Eng. Chem. 3(4), 324 (1964).

APPENDIX - 1

Calculation for uniform temperature assumption justification of copper bead:

Thermal conductivity of copper = 385.33 W/m.K

Specific heat of copper = 385.2 J/Kg.K

Density of copper = 8.92×10^3 kg/m^3

Radius of bead = 1.75×10^{-3} m

$$\therefore \text{ Thermal diffusivity} = \frac{385.33}{8.92 \times 10^3 \times 385.2} = 1.12 \times 10^{-4} \text{ m}^2/\text{s}$$

As the residence time of bead infront of the heater is 0.25 s.

$$Fo = \frac{1.12 \times 10^{-4} \times 0.25}{(1.75 \times 10^{-3})^2} = 9.14$$

$$\text{Hence } \frac{1}{50} Fo = 0.183$$

Taking maximum heat transfer coefficient in water to be 2834.57 w/m^2.k (500 Btes/ft^2.hr °F)

$$Bi = \frac{2834.57 \times 1.75 \times 10^{-3}}{385.33} = 1.3 \times 10^{-2}.$$